Universitat Politècnica de Catalunya
Departamento de Teoría de la Señal y Comunicaciones

TESIS PARA LA OBTENCIÓN DEL TÍTULO DE DOCTOR INGENIERO DE TELECOMUNICACIÓN.

Sistemas Lidar coherentes e incoherentes de baja potencia para la detección de velocidad de blancos sólidos.

Alejandro Rodríguez Gómez

Directores: Dr. Adolfo Comerón Tejero
Dr. Antoni Elias Fusté.

Mayo 1998.

3. Líneas futuras.

En este capítulo se describen algunas de las líneas futuras en el campo de los sistemas lidar. Algunas de ellas ya han sido brevemente exploradas y serán objeto de atención de la actividad del autor y de otros miembros del grupo de trabajo de lidar de la Universitat Politècnica de Catalunya. Como se puede comprobar, están centradas fundamentalmente en los sistemas coherentes.

3.1. SISTEMAS HETERODINOS.

Uno de los principales limitaciones de la detección homodina, empleada por el lidar coherente descrito en la parte II, es su incapacidad para discriminar el signo de la velocidad. Así, el sistema es incapaz de distinguir si el desplazamiento Doppler es positivo o negativo: en ambos casos la frecuencia de la modulación en amplitud que aparece en la envolvente de la onda descrita en la ecuación (I.69) será del módulo de la diferencia frecuencial $\Delta\omega$ entre el oscilador local, y por tanto de la señal transmitida, y de la señal recibida.

Esta situación no es ajena a los sistemas radar en general, y la estrategia habitual es emplear receptores heterodinos (*superheterodinos*). En un receptor heterodino la frecuencia del oscilador local está desplazada un valor ω_{FI} conocido respecto de la portadora transmitida. Ello implica que

para un desplazamiento Doppler nulo, el batido entre señales producirá una envolvente de frecuencia igual a $|\omega_{FI}|$. Habitualmente se elige un valor de ω_{FI} de valor absoluto superior al del mayor desplazamiento Doppler esperable.

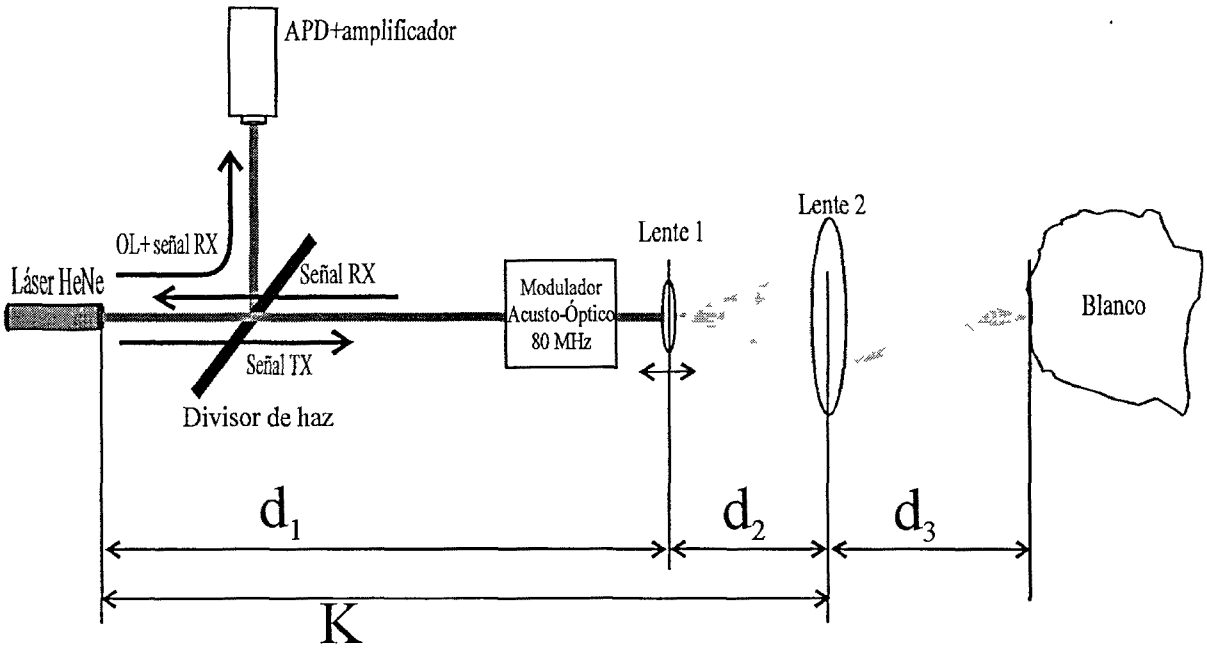

Figura IV.8. Subsistema óptico de un lidar coherente heterodino.

En el laboratorio se han realizado algunas pruebas preliminares con un sistema heterodino basado en el lidar coherente de la parte II y que se puede ver en la figura IV.8. Se ha procedido a desplazar tanto la señal transmitida como la recibida, empleando un modulador acusto-óptico modelo ISOMET 1205C [Isomet, 88] como desplazador frecuencial. Este desplazador produce un desplazamiento de $\pm 80 \cdot n$ *MHz*, con n entero, para un ángulo de entrada del haz igual a $\pm n$ veces el ángulo de Bragg [Saleh-Teich, 91]. Por lo tanto la frecuencia intermedia conseguida es de $\pm 160 \cdot n$ *MHz*, dado que la luz atraviesa el dispositivo dos veces.

Para el dispositivo empleado, el ángulo de Bragg asociado a la componente fundamental es de $\theta_B = 7$ *mrad* (*0,4°*), lo que implica un pequeñísimo desplazamiento respecto de la coaxialidad del sistema homodino. En el prototipo probado en el laboratorio se ha obviado esta circunstancia, absorbiéndose en las tolerancias de posición de los diferentes elementos ópticos. No obstante, en un sistema definitivo es interesante tener en cuenta este ángulo y construir una estructura rígida tubular que lo incluya, a fin de no provocar desapuntamientos. En la figura IV.9 se han representado las medidas de frecuencia de la señal Doppler detectada, obtenidas con un analizador de espectros, para velocidades positivas y negativas, para un ángulo $\varphi = 30°$.

Sobre el efecto acusto-óptico se puede encontrar información básica en la referencia [Saleh-Teich, 91] y más detallada en [Korpel, 88].

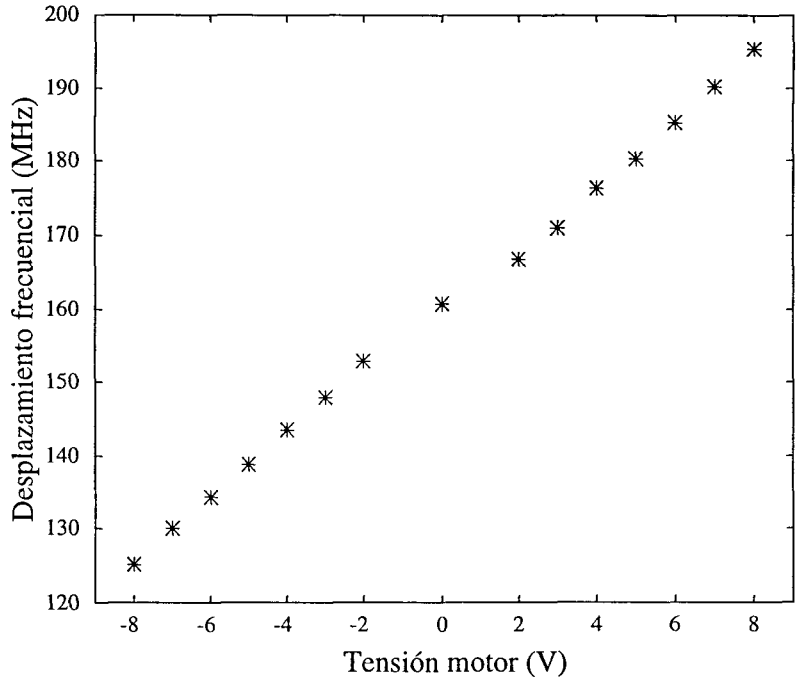

Figura IV.9. Frecuencia de la señal Doppler frente a velocidad angular de giro del blanco rotatorio.

3.2. SISTEMAS COHERENTES BASADOS EN LÁSER DE SEMICONDUCTOR Y ÓPTICA GUIADA.

El empleo de sistemas en óptica guiada proporciona una robustez muy deseable en sistemas comerciales. No obstante, el precio de los diodos láser (fuente láser más adecuada para trabajar con sistemas en fibra) con valores de coherencia temporal adecuados a las necesidades de los sistemas coherentes es aún caro.

3.2.1. Sistemas con mezcla en el propio diodo láser.

Las referencias [Rudd, 68] y [Churnside, 84a] ya proponían sistemas en óptica no guiada en los que el láser transmisor actúa, además, como mezclador. No obstante, el sistema de Rudd, de acuerdo con la referencia [Potter, 69], tiene una respuesta frecuencial que no llega a los *100 kHz*, lo que lo imposibilita medir velocidades superiores a algunos centímetros por segundo. El sistema de Churnside, sin embargo, trabaja con un láser de CO_2, cuya respuesta frecuencial es mucho más amplia, de unos *10 MHz*, lo que permite, para una longitud de onda de *10* μm, medir velocidades superiores a *50 m/s*.

Diferentes autores ([Mul, 84], [Shinohara, 86], [Koelink, 92] y otros) han comunicado sistemas basados en diodo láser en los que la mezcla óptica se produce en el propio diodo. La mayor parte de ellos suelen detectar la modulación en amplitud en el fotodiodo que suele acompañar en el

encapsulado a los diodos láser para monitorizar la potencia transmitida, o bien en la influencia que produce en la tensión de alimentación.

3.2.2. Sistemas con mezcla en un fotodiodo externo.

Se trata de la evolución natural de los sistemas coherentes desarrollados en el presente trabajo. Consiste en la reproducción del subsistema óptico empleado en el prototipo descrito en la parte II con elementos desarrollados en fibra óptica monomodo mantenedora de polarización. El mayor inconveniente que presentan estos sistemas es, una vez más, el alto precio de los diferentes componentes.

El sistema estaría basado en el mezclador en fibra presentado en el apartado I.5.6.2, en la figura I.30. En la figura IV.10 se presenta una modificación del anterior que incluye un modulador acusto-óptico con entrada y salida en fibra, lo que permitiría la recepción heterodina.

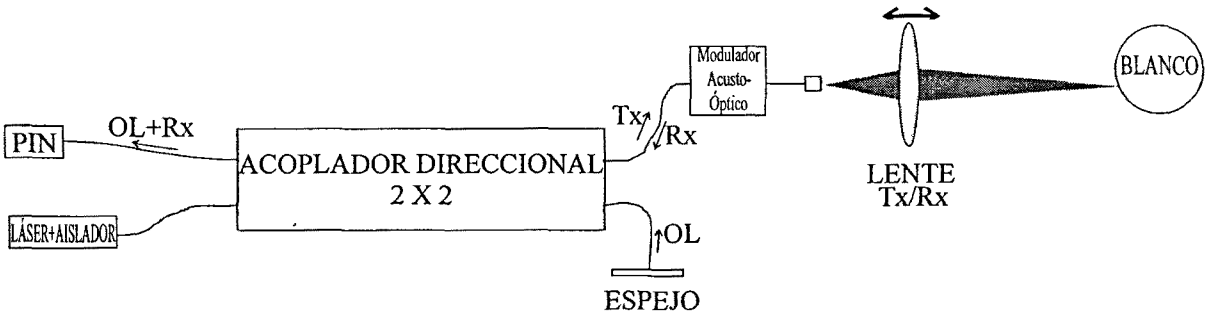

Figura IV.10. Prototipo de lidar coherente heterodina en fibra con mezcla en el fotodiodo.

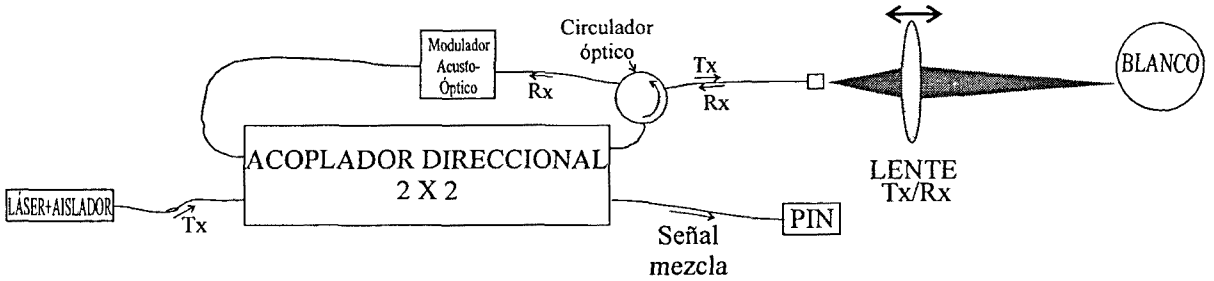

Figura IV.11. Prototipo lidar coherente heterodino en fibra con mezcla en el propio diodo láser transmisor y detección en un fotodiodo externo.

Otra alternativa posible es la que se presenta en la figura IV.11, en el que se emplea un circulador óptico para separar el camino de transmisión y recepción. Además, nos permite cambiar la ubicación del modulador acusto-óptico, con lo que la frecuencia intermedia del sistema heterodino es igual a la frecuencia fundamental de éste.

3.3. SISTEMAS PULSADOS COHERENTES. APLICACIÓN A ESTUDIO DE LA ATMÓSFERA.

Otra de las actividades futuras en el grupo es la de los sistemas para medida de vientos. En la referencia [Huffaker, 96] pueden encontrarse diferentes sistemas en funcionamiento actualmente.

El esquema básico parte del concepto de radar meteorológico [Doviak, 84]; en el lidar, sin embargo, el procesado espectral no se realiza a partir de ecos procedentes de diferentes pulsos, sino en la señal procedente de un único eco. Esto es debido a que, a diferencia de lo que ocurre en los sistemas radar de microondas, no existe referencia común de fase entre los sucesivos pulsos obtenidos de un láser que funcione con mecanismos como el Q-switching, o incluso en estructuras Master Oscillator Power Amplifier (MOPA) con modulación a bajo nivel. En este sentido se han propuesto sistemas que emplean láseres pulsados mediante mode-locking, en los que sí hay continuidad en la referencia de fase entre pulsos [Gordienko, 91].

El esquema de la óptica del sistema es el que aparece en la figura IV.12. Como se puede apreciar, el aislamiento entre señal transmitida y recibida se consigue empleando diferente polarización (circular de sentidos contrarios). Para ello se emplea un prisma Glan y una lámina en $\lambda/4$. Se emplea un telescopio como óptica de transmisión/recepción. El oscilador local se obtiene generalmente del seeder del láser transmisor, o bien de otro oscilador maestro. La mezcla se realiza empleando un acoplador direccional en fibra monomodo mantenedora de polarización.

A diferencia del lidar coherente de baja potencia desarrollado en este trabajo, se trata de un sistema enfocado al infinito.

En la tabla IV.1 se han recogido los parámetros básicos del sistema. De acuerdo con éstos, se han realizado cálculos de la relación señal Doppler a ruido para sistemas con diferentes valores de apertura de transmisión/recepción. Los resultados se han representado en la figura IV.13

-Energía por pulso:	*20 mJ*
-Longitud de onda:	*1,064 μm*
-Potencia de oscilador local:	*1 mW*
-Responsividad fotodiodo:	*0,19 A/W*
-Ganancia de transimpedancia:	*10 kΩ*
-Datos atmósfera:	
Atenuación (α):	$1{,}2 \cdot 10^{-4}$ *dB/km*
Retrodispersión (β):	10^{-6} $km^{-1} \cdot sr^{-1}$

Tabla IV.1. Características del Lidar Coherente Atmosférico bajo estudio [Montero, 98].

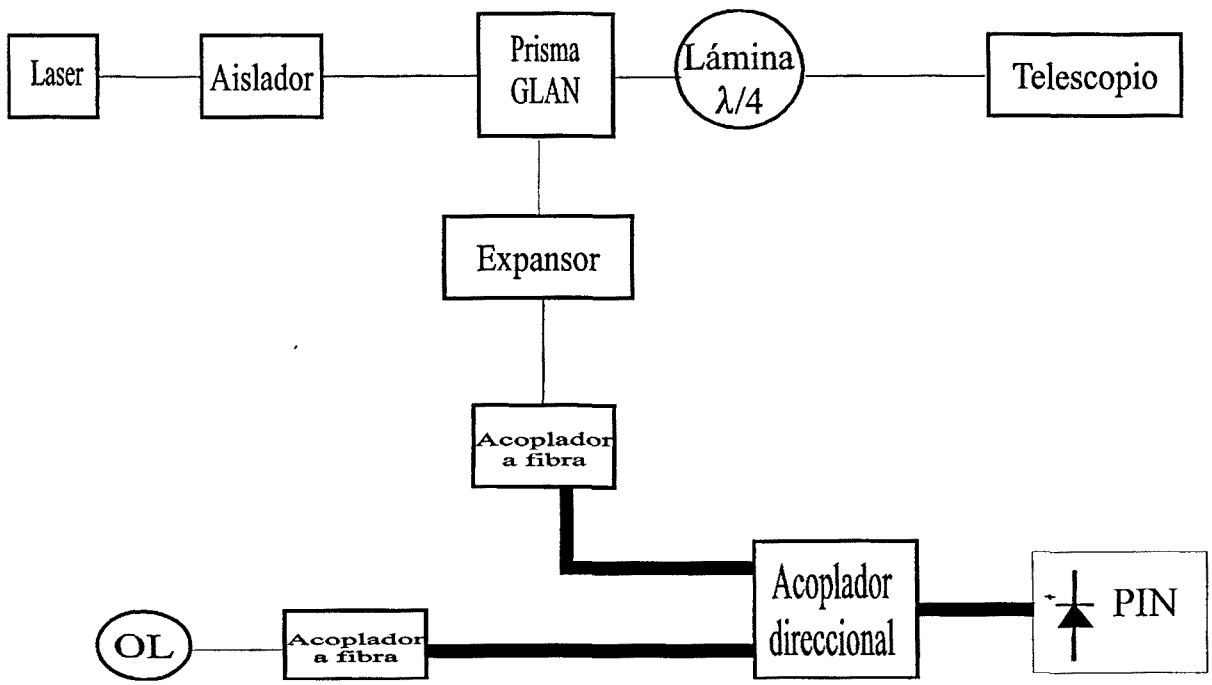

Figura IV.12. Prototipo lidar coherente para medida de vientos [Montero, 98].

Así, se han considerado aperturas de *1, 5, 10, 15* y *20 cm* de diámetro. Los cálculos se han realizado teniendo en cuenta los efectos de retrodispersión y atenuación en la atmósfera (para unos valores de retrodispersión $\beta = 10^{-6} km^{-1} sr^{-1}$ y de atenuación atmosférica $\alpha = 10\ km$). También se ha tenido en cuenta los efectos de coherencia espacial descritos en el capítulo I.4. De los cálculos realizados se deduce que la apertura más adecuada para este sistema es la de *10 cm* de diámetro. Exigiendo un mínimo de relación señal a ruido de *5 dB*, el alcance del sistema es de unos *3 500 m.* Los cálculos realizados para valores de apertura mayores de *20 cm* de diámetro dan como resultado alcances menores.

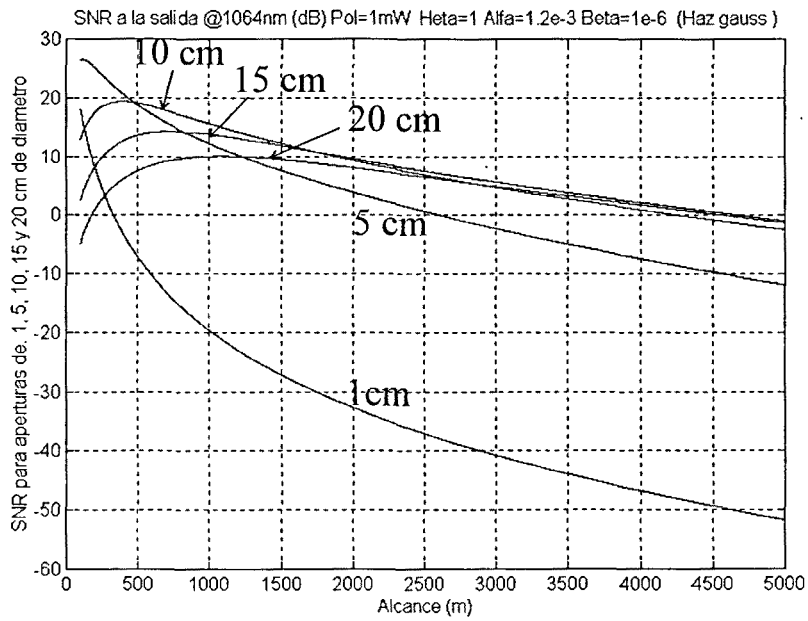

Figura IV.13. Relación señal a ruido frente a distancia en un lidar coherente pulsado para medida de vientos con las características recogidas en la tabla IV.11, para diferentes valores de diámetro de las aperturas de transmisión/recepción [Montero, 98].

Bibliografía

[Aguasca, 96] Albert Aguasca i Solé, Comunicación privada, enero 1996.

[Analog, 94] Catálogo de Analog Modules, 1994.

[Andrés, 98] Mª Dolores Andrés Alcalde, *Sistema Lidar Pulsado Incoherente para Detección de Blancos Sólidos*. Proyecto Fin de Carrera. Director: Alejandro Rodríguez Gómez, ETSETB, 1998.

[Ares, 95] Carlos Ares Grondona, *Sistema de diodo laser de uso general para laboratorio*. Proyecto Fin de Carrera. Director:Adolfo Comerón Tejero, ETSETB, 1995.

[Bachman, 79] Christian G. Bachman, *Laser Radar Systems and Techniques*, Artech House, Dedham MA (USA), 1979.

[Avtech, 95] AVTECH, *Catalog no. 9*, Avtech Electrosystems, 1995

[Bordes, 98] Núria Bordes, *Sistema fotorreceptor para lidar coherente*, Proyecto Fin de Carrera. Director: Alejandro Rodríguez Gómez, ETSETB, 1998.

[Born&Wolf, 80] M. Born, E. Wolf, *Principles of Optics*, Pergamon Press, New York, 6th edition, 1980.

[Burle, 90] BURLE, *Photomultipliers*, Catalog, 1990.

[Carmer, 96] Dwayne C. Carmer, Lauren M. Peterson, "Laser Radar in Robotics", *Proceedings of the IEEE*, Vol. 84, No. 2, February 1996, pp. 299-320.

[Churnside, 82] J.H. Churnside, "Speckle from a rotating diffuse object", *J. Opt. Soc. Am.*, Vol. 72, No. 11, November 1982, pp. 1464-9.

[Churnside, 84a] J.H. Churnside, "Laser Doppler Velocimetry by modulating a CO_2 laser with backscattered light", *Applied Optics*, Vol. 23, No. 1, pp 61-6.

[Churnside, 84b] J.H. Churnside, "Signal-to-noise in a backscattered-modulated Doppler velocimeter", *Applied Optics*, Vol. 23, No. 13, pp 2097-2106.

[Clark, 93] Robert S. Clark, "Avalanche photodiode: low-light challenge to the photomultiplier tube", *OE Reports*, No.119, Nov. 1993.

[Comlinear, 93] Comlinear Corporation, *Solutions with Speed 1993-94.*

[Crowe, 93] Devon G. Crowe, Paul R. Norton, Thomas Limperis, Joseph Mudar, "Detectors" in *Electro-Optical Components*, William D. Rogatto, editor, *The Infrared & Electro-Optical Systems Handbook*, Joseph S. Accetta, David L. Shumaker, executive editors, ERIM-SPIE, 1993.

[Dainty, 84] J.C. Dainty, editor, *Laser Speckle and Related Phenomena*, Springer-Verlag, 1984.

[Dautet, 93] Henri Dautet, et al. "Photon counting techniques with silicon avalanche phtodiodes", *Applied Optics*, Vol. 32, No. 21, July 1993.

[Degnan, 74] John Degnan, Bernard J. Klein, "Optical Antenna Gain. 2: Receiving Antennas", *Applied Optics*, Vol. 13, No. 10, pp. 2397-2401.

[Dios, 97] Federico Dios, Alejandro Rodríguez, et al., *Realización de sistemas láser portátiles de medida de velocidad por efecto Doppler (LDA-LDV) de bajo coste para aplicaciones industriales e hidrodinámicas*, propuesta PETRI 95-0249-OP, Noviembre 1997.

[Doviak, 84] Richard J. Doviak, Dusan S. Zrnić, *Doppler Radar and Weather Observations*, Academic Press, San Diego (CA, USA), 1984.

[Drain, 80] L.E. Drain, *The Laser Doppler Technique*, John Wiley & Sons, Norwich (GB), 1980.

[EG&G, 92] Catálogo de fotodiodos, APDs y diodos láser.

[Feynman, 63] R.P. Feynman, R. B Leighton, M. Sands, *The Feynman Lectures on Physics, Vol. I. Mainly Mechanics, Radiation and Heat*, Addison-Wesley, 1963.

[Fisher, 92] P. David Fisher, "Improving on police radar", *IEEE Spectrum*, July 1992, pp. 38-43.

[Frehlich, 91] Rod G. Frehlich, "Coherent laser radar performance for general atmospheric refractive turbulence", *Applied Optics*, Vol. 30, no. 6, pp. 5325-52.

[Frehlich, 93] Rod G. Frehlich, "Optimal local oscillator field for a monostatic coherent laser radar with a circular aperture", *Applied Optics*, Vol. 32, No. 24, 20 August 1993, pp. 4569-77.

[Fried, 67] David L. Fried, "Optical Heterodyne Detection of an Atmospherically Distorted Signal Wave Front", *Proceedings of the IEEE*, Vol. 55, no. 1, January 1967, pp. 57-67.

[Galán, 97] Miguel Galán, Comunicación privada, Junio 1997.

[Gaussorgues, 94] G. Gaussorgues, *Infrared Thermography*, Chapman & Hall, 1994.

[González, 95] Enrique González Terceño, *Optimización y medidas de un sistema Lidar coherente para medición de velocidades de blancos sólidos*. Proyecto Fin de Carrera. Director: Alejandro Rodríguez Gómez, ETSETB, 1995.

[Goodman, 84] J.W. Goodman, "Statistical Properties of Laser Speckle Patterns", Chap. 2 in *Laser Speckle and related phenomena*, edited by J.C. Dainty, Springer-Verlag, 1984.

[Goodman, 85] J.W. Goodman, *Statistical Optics*, John Wiley & Sons, New York (NY, USA), 1985.

[Gordienko, 91] V.M. Gordienko et al, "Infrared coherent lidar systems for wind velocity measurements", *Laser Radar VI*, Richard J. Becherer, editor, Proc SPIE 1416.

[Guth, 97] Reinhold Guth, "A Designer's Guide to Photomultipliers", *EuroPhotonics*, June/July 1997, pp. 57-8.

[Hamamatsu, 93] HAMAMATSU, *Electron Tube Products*, Condensed Catalog '93.

[Hargert, 96] Earl Hargert and Craig Walling, "Photomultiplier Tubes See the Light - One Photon at a Time", *Photonics Spectra*, December 1996, pp.98-102.

[He, 91] X.D. He, K.E. Torrance, "A Comprehensive Physical Model for Light Reflection", *Computer Graphics*, Vol. 25, No. 4, 1991, pp. 175-186.

[Hecht, 92] Jeff Hecht, *The Laser Guidebook*, Second Edition, McGraw-Hill, New York, 1992

[Hecht, 94] Jeff Hecht, *Understanding Lasers*, 2nd ed., IEEE Press, New York NY(USA), 1994.

[Henry, 82] Charles H. Henry, "Theory of the Linewidth of Semiconductor Lasers", *IEEE Journal of Quantum Electronics*, Vol. QE-18, no. 2, Feb. 1982, pp. 259 ss.

[Herman, 97] Hervé-Yves Herman, Comunicación privada, Julio 1997.

[Herranz, 80] Guillermo Herranz Acero, *Convertidores electromecánicos de energía*, Marcombo Boixareu, 1980.

[Higgins, 95] Thomas V. Higgins, "The three phases of lasers: solid-state, gas and liquid", *Laser Focus World*, July 1995, pp. 73-85.

[Hinkley, 76] E.D. Hinkley, ed., *Laser Monitoring of the Atmosphere*, Springer-Verlag, New York, 1976.

[Huffaker, 70] R.M. Huffaker, A.V. Jelalian, J.A.L. Thomson, "Laser-Doppler System for Detection of Aircraft Trailing Vortices", *Proceedings of the IEEE*, Vol. 58, No.3, March 1970, pp. 322-6.

[Huffaker, 96] R.M.Huffaker, R.M. Hardesty, "Remote Sensing of Atmospheric Wind Velocities Using Solid-State and CO_2 Coherent Laser Systems", *Proceedings of the IEEE*, Vol.84, no.2, Feb. 1996, pp. 181-204.

[Isomet, 88] *1205C Acousto-Optic Modulator*, ISOMET Corporation, April 1988.

[Jammers, 98] Jammers, Inc. "We help you vanish from police radar and laser speed guns", http://www.car-trek.com/jammers/, documento Web, enero 1998.

[Jelalian, 92] Albert V. Jelalian, *Laser Radar Systems*, Artech House, Norwood MA(USA), 1992

[Klein, 74] Bernard J. Klein, John J. Degnan, "Optical Antenna Gain. 1: Transmitting Antennas", *Applied Optics*, Vol. 13, No. 9, Sept 1974, pp. 2134-41.

[Kamas, 77] George Kamas, ed., *Time and Frequency Users' Manual*, National Bureau of Standards, U.S. Department of Commerce, May 1977.

[Klein, 76] Bernard J. Klein, John J. Degnan, "Optical Antenna Gain. 3: The effect of secondary element support struts on transmitter gain", *Applied Optics*, Vol. 15, No. 4, April 1976, pp. 977-9.

[Koelink, 92] M.H. Koelink, et al, "Laser Doppler velocimeter based on the self-mixing effect in a fiber-coupled semiconductor laser: theory", *Applied Optics*, Vol.31, No. 18, June 1992, pp. 3401-8.

[Kompa, 84] G. Kompa, "Optical short-range radar for level control measurement", IEE Proceedings, Vol. 131, Pt. H, No.3, June 1984.

[Korpel, 88] Adrian Korpel, *Acousto-optics*, New York M. Dekker, 1988.

[Lerner, 96a] Eric J. Lerner, "Photomultiplier tubes offer high-end sensitivity", *Laser Focus World*, July 1996, pp. 87-96.

[Lerner, 96b] Eric J. Lerner, "Avalanche photodiodes can count the photons", *Laser Focus World*, October 1996, pp. 93-102.

[López, 95] Carmen López Martínez, *Modelos para el cálculo de la Sección Recta Radar Láser (LRCS) de blancos sólidos.* Proyecto Fin de Carrera. Director: Alejandro Rodríguez Gómez, ETSETB, 1995.

[Measures, 84] Raymond M. Measures, *Laser Remote Sensing*, Krieger, Malabar FL(USA), 1984.

[Melle, 95] Serge Melle, Andrew MacGregor, "How to choose avalanche photodiodes", *Laser Focus World*, October 1995, pp. 145-156.

[Melles-Griot, 95] *Optics, Opto-mechanics, Lasers, Instruments*, Catálogo general Melles-Griot, 1995/96.

[Melngailis, 96] Ivars Melngailis, et al, "Laser Radar Component Technology", *Proceedings of the IEEE*, Vol. 84, no. 2, February 1996, pp. 227-267.

[Mesalles, 98] Eloy Mesalles Nalda, *Subsistema de adquisición y medida para un lidar coherente CW*, Proyecto Fin de Carrera. Directores: Adolfo Comerón Tejero y Alejandro Rodríguez Gómez, ETSETB, 1998.

[Mirsky, 78] G. Mirsky, *Radioelectronic Measurements*, 1st edition in English, Mir, 1978.

[Montero, 98] José Alberto Montero, *Estudio del sistema óptico para un Lidar Coherente Atmosférico*. Proyecto Fin de Carrera. Director: Alejandro Rodríguez Gómez, ETSETB, 1998.

[Montesino, 94] José Luis Montesino-Espartero Ripol, *Desmodulador coherente a frecuencias ópticas con aplicaciones a LIDAR.* Proyecto Fin de Carrera. Director: Alejandro Rodríguez Gómez, ETSETB, 1994.

[Mooradian, 85] Aram Mooradian, "Laser linewidth", *Physics Today*, May 1985, pp. 43 -8.

[Möller, 88] K.D. Möller, *Optics*, Mill Valley, C.A. University Science Books.

[Mul, 84] F.F.M. de Mul, et al, "Mini laser-Doppler (blood) flow monitor with diode laser source and detection integrated in the probe", *Applied Optics*, Vol.23, No. 17, September 1984, pp. 2970-3.

[New Focus, 97] *New Focus, 1997/98 Catalog.*

[Newport, 94] *The 1994 Newport Catalog.*

[Newport, 96] *Photonics, 1996 Catalog*, Newport.

[Oriel, 94] *Light Sources*, Catálogo general Oriel, Vol. II, Oriel, 1994.

[OSA, 95] Topical Meeting on *Coherent Laser Radar: Technology and Applications, 1995,* July 23-27, 1995, Keystone, Colorado (USA), sponsored by Optical Society of America (OSA), Postconference edition.

[Osche, 96] Gregory R. Osche, Donald S. Young, "Imaging Laser Radar in the Near and Far Infrared", *Proceedings of the IEEE*, Vol. 84, No.2, February 1996.

[Osiński, 87] Marek Osiński, Jens Buus, "Linewidth Broadening Factor in Semiconductor Lasers - An Overview", *IEEE Journal of Quantum Electronics*, Vol. QE-23, no. 1, Jan. 87, pp. 9 ss.

[Papoulis, 80] Athanasios Papoulis, *Probabilidad, variables aleatorias y procesos estocásticos*, Editorial Universitaria de Barcelona, 1980.

[Pedret, 88] *Optic's*, Catálogo de óptica, Industrias Pedret, marzo 1988.

[Piskarkas, 97] Algis P. Piskarkas, "Optical Parametric Generators: Tunable, Powerful & Ultrafast", *Optics & Photonics News*, Optical Society of America (OSA), Vol. 8, No. 7, July 1997, pp. 25 ss.

[Pons, 93] Pablo Pons y Torres, *Manual Ilustrado del Reglamento de Circulación y Seguridad Vial*, Pons Editorial, 1993.

[Potter, 69] I.C. Potter, "Frequency Response of the 6328-Å Helium-Neon Laser Interferometer", *Journal of Applied Physics*, Vol. 40, no. 12, nov. 1969, pp. 4770-6.

[Queija, 94] Gabino Rodríguez Queija, *Antena Óptica para Lidar Coherente*, Proyecto Fin de Carrera. Director: Alejandro Rodríguez Gómez, ETSETB, 1994.

[RCA-C30902E] RCA Inc. Electrooptics, *Photodiode C30902E, C30902S, C30921E, C30921S.*

[RCA-C30954E] RCA Inc. Electrooptics, *Photodiode C30954E, C309055E, C30956E.*

[Rocadenbosch, 96] Francesc Rocadenbosch Burillo, *LIDAR Sensing of the Atmosphere*, Tesis doctoral, director: Adolfo Comerón Tejero. Universitat Politècnica de Catalunya, 1996.

[Rodríguez, 95a] Alejandro Rodríguez, Adolfo Comerón, Enrique González, Antoni Elias, "Traffic Monitoring: The Coherent Laser Radar Approach", *Microwave Engineering Europe*, March-April 1995, pp. 29-34.

[Rodríguez, 95b] Alejandro Rodríguez, Adolfo Comerón, Enrique González, J.L. Montesino-Espartero, Gabino Rodríguez, "Low-cost, low power Laser Doppler Velocimetry with applications to traffic monitoring",in *Law Enforcement Technologies: Identification Technologies and Traffic Safety*, Bernard Dubuisson, Geoffrey Harding, chairs/editors, Proceedings of the SPIE, vol. 2511, paper 2511-22.

[Rodríguez, 95c] Alejandro Rodríguez, Adolfo Comerón, Antoni Elias, Enrique González, José Luis Montesino-Espartero, Gabino Rodríguez, "Low-power coherent laser radar velocimeter: applications to law enforcement", 25th European Microwave Conference, paper 487/C 4.2. Bologna, Italia, 4-8 septiembre 1995, pp. 485-489.

[Rodríguez, 95d] Alejandro Rodríguez, Adolfo Comerón, Antoni Elias, Enrique González, José Luis Montesino-Espartero y Gabino Rodríguez, "Velocímetro radar laser coherente de baja potencia: aplicaciones a control de tráfico". *URSI 95*, Sesión D9(1) Valladolid, 27-29 de septiembre 1995, pp. 797-800.

[Rodríguez, 95e] Alejandro Rodríguez, Carmen López y Adolfo Comerón, "Modelos para el cálculo de la sección recta lidar (LCRS) de blancos sólidos", *URSI 95*, Sesión D9(2), Valladolid, 27-29 septiembre 1995, pp. 825-828.

[Rodríguez, 97a] Alejandro Rodríguez, Adolfo Comerón, Albert Aguasca Solé, Eloy Mesalles Nalda, Carles Puente Baliarda, Francesc Rocadenbosch Burillo, "Sistema Lidar Coherente para Monitorización de Velocidades de Blancos Sólidos", URSI '97, Bilbao, 1997.

[Rodríguez, 97b] Alejandro Rodríguez, Adolfo Comerón, Mª Dolores Andrés Alcalde, Verónica Tercero Vargas, Carles Puente Baliarda, Francesc Rocadenbosch Burillo, "Sistema Lidar Incoherente para Medida de Distancia y Velocidad de Blancos Sólidos , URSI '97, Bilbao, 1997.

[Rogatto, 93] William D. Rogatto, ed., *Electro-Optical Components*, Vol. 3 de *The Infrared & Electro-Optical Systems Handbook*, ERIM & SPIE, 1993.

[Rombaut, 95] M. Rombaut, N. Le Fort-Piat, "Intelligent onboard system for driver assistance" in *Law Enforcement Technologies: Identification Technologies and Traffic Safety*, Proceedings of the SPIE, vol. 2511, paper 2511-25.

[Rudd, 68] M.J. Rudd, "A laser Doppler velocimeter employing the laser as a mixer-oscillator", *Journal of Scientific Instruments (Journal of Physics E)*, Series 2 Volume I, 1968, pp. 723-6.

[Rupérez, 93] Mª José Rupérez, "Normativa Comunitaria aplicable a láseres. La seguridad frente a radiación láser: Norma EN 60 825 (1992)", *Salud y Trabajo*, nº 97, 1993, pp. 11-17.

[Rye, 82] Barry J. Rye, "Primary aberration contribution to incoherent backscatter heterodyne lidar returns", *Applied Optics*, Vol. 21, No. 5, 1 March 1982, pp. 839-844.

[Rye, 92] Barry J. Rye and Rod G. Frehlich, "Optimal truncation and optical efficiency of an apertured coherent lidar focused on an incoherent backscatter target", *Applied Optics*, Vol. 31, No. 15, 20 May 1992, pp. 2891-9.

[Sáiz, 94] Magdalena Sáiz Rodrigo, "Optical 'speedometer' to monitor Spain's traffic", *Opto & Laser Europe*, September '94, pp 32-33.(1994)

[Saleh-Teich, 91] B.E.A. Saleh, M.C. Teich, *Fundamentals of Photonics*, John Wiley & Sons, 1991.

[SDL , 94] *1994 Laser Diode Product Catalog*, SDL, 1994.

[Senior, 85] John M. Senior, *Optical Fiber Communications. Principles and Practice*, Prentice-Hall, 1985.

[Shinohara, 86] S. Shinohara, et al, "Laser Doppler velocimeter using the self-mixing effect of a semiconductor laser diode", *Applied Optics*, Vol. 25, No. 9, May 1986, pp. 1417-9.

[Siegman, 66] A.E. Siegman, "The Antenna properties of optical heterodyne receivers", *Proceedings of the IEEE*, Vol. 54, no. 10, october 1966, pp. 1350-6.

[Siegman, 86] A.E. Siegman, *Lasers*, University Science Books, 1986.

[Siemens, 89] *Helium-Neon Laser Tubes, Modules and Power-Supplies, 1989/90*, SIEMENS, 1989.

[Skolnik, 80] Merrill I. Skolnik, *Introduction to Radar Systems*, McGraw-Hill, 1980.

[Sliney, 80] David Sliney, Myron Wolbarsht, *Safety with Lasers and Other Optical Sources*, Plenum Press, New York, 1980.

[Smith, 90] Warren J. Smith, *Modern Optical Engineering*, McGraw-Hill, 1980.

[Solà, 95] Ricard Solà Casanoves, *Radar Laser Polsat per la mesura de velocitat i contorns de vehícles.* Proyecto Fin de Carrera. Director:Prof. Dr.-Ing. Gunter Kompa, ETSETB, 1995.

[SPIE, 96] *Laser radar technology and applications*, Gary W. Kamerman chair/editor, Proceedings of the SPIE, vol. 2748, 1996.

[Stann, 96] Barry L. Stann et al., "Intensity-modulated diode laser radar using frequency-modulation/continuous-wave ranging techniques", *Optical Engineering*, Vol. 35(11), pp. 3270-8.

[Teich, 68] M.C. Teich, "Infrared Heterodyne Detection", *Proceedings of the IEEE*, Vol. 56, No. 1, pp. 37-46.

[Uniphase, 85] *Novette, Model 1500 Series Helium-Neon Lasers*, Uniphase, 1985.

[Vampola, 93] John L. Vampola, "Readout Electronics for Infrared Sensors" in *Electro-Optical Components*, William D. Rogatto, editor, *The Infrared & Electro-Optical Systems Handbook*, Joseph S. Accetta, David L. Shumaker, executive editors, ERIM-SPIE, 1993.

[Verly, 96] Jacques G. Verly, Richard L. Delanoy, "Model-Based Automatic Target Recognition (ATR) System for Fordwardlooking Groundbased and Airborne Imaging Laser Radars", *Proceedings of the IEEE*, Vol. 84, No. 2, February 1996, pp. 126-163.

[White, 96] Ian White, "Picosecond Optical Pulse Generation Using Semiconductor Lasers", Majid Ebrahimzadeh, "Pulsed Parametric Oscillators", Wilson Sibbet "Ultrashort Pulsed Sources" in *Lasers Sources and Applications*, A.Miller, D.M.Finlayson, eds., Proceedings of the 47th SUSSP, SUSSP & Institute of Physics Publishing, Bristol-Philadelphia, 1996.

[Yariv, 89] Amnon Yariv, *Quantum Electronics*, 3rd edition, John Wiley, 1989.

Apéndices

A.1. Especificaciones del fotodiodo C30902E.

EG&G OPTOELECTRONICS

22001 Dumberry Road
Vaudreuil, Quebec
J7V 8P7
Tel.: (514) 424-3300 Fax: (514) 424-3411

Silicon Avalanche Photodiodes

C30902E, C30902S, C30921E, C30921S

DATA SHEET

High Speed Solid State Detectors for Fiber Optic and Very Low Light-Level Applications

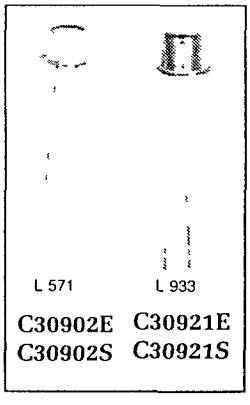

RCA Type C30902E avalanche photodiode utilizes a silicon detector chip fabricated with a double-diffused "reach-through" structure. This structure provides high responsivity between 400 and 1000 nanometers as well as extremely fast rise-and falltimes at all wavelengths. Because the fall-time characteristics have no "tail", the responsivity of the device is independent of modulation frequency up to about 800 MHz. The detector chip is hermetically-sealed behind a flat glass window in a modified TO-18 package. The useful diameter of the photosensitive surface is 0.5 mm.

RCA Type C30921E utilizes the same silicon detector chip as the C30902E, but in a package containing a lightpipe which allows efficient coupling of light to the detector from either a focussed spot or an optical fiber up to 0.25 mm in diameter. The internal end of the lightpipe is close enough to the detector surface to allow all of the illumination exiting the lightpipe to fall within the active-area of the detector. The hermetically-sealed TO-18 package allows fibers to be epoxied to the end of the lightpipe to minimize signal losses without fear of endangering detector stability.

The C30902E and C30921E are designed for a wide variety of uses including optical communications at data rates to 1 GBit/second, laser range-finding, and any other applications requiring high speed and/or high responsivity.

The C30902S and C30921S are selected C30902E and C30921E photodiodes having extremely low noise and low bulk dark-current. They are intended for ultra-low light level applications (optical power less than 1 pW) and can be used in either their normal linear mode ($V_R<V_{BR}$) at gains up to 250 or greater, or as photon counters in the "Geiger" mode ($V_R>V_{BR}$) where a single photoelectron may trigger an avalanche pulse of about 10^8 carriers. In this mode, no amplifiers are necessary and single-photon detection probabilities of up to approximately 50% are possible.

Photon-counting is also advantageous where gating and coincidence techniques are employed for signal retrieval.

- **High Quantum Efficiency**
  77% Typical at 830 nm
- **C30902S and C30921S in Geiger Mode:**
  - **Single-Photon Detection Probability to 50%**
  - **Low Dark-Count Rate at 5% Detection Probability – Typically**
    15,000/second at +22° C
    350/second at -25° C
  - **Count Rates to 2×10^6/second**
- **Hermetically Sealed Package**
- **Low Noise at Room Temperature**
  - **C30902E, C30921E –**
    2.3×10^{-13} A/Hz$^{1/2}$
  - **C30902S, C30921S –**
    1.1×10^{-13} A/Hz$^{1/2}$
- **High Responsivity –**
  Internal Avalanche Gains in Excess of 150
- **Spectral Response Range – (10% Points)**
  400 to 1000 nm
- **Time Response – Typically 0.5 ns**
- **Wide Operating Temperature Range –**
  -40° C to +70° C

Optical Characteristics

C30902E, C30902S (Figure 13)

Photosensitive Surface:

Shape	Circular	
Useful area	0.2	mm^2
Useful diameter	0.5	mm

Field of View:

Approximate full angle for totally illuminated photosensitive surface	100	deg

C30921E, C30921S (Figure 14)

Numerical Aperture of Light Pipe	0.55	
Refractive Index (n) of Core	1.61	
Light Pipe Core Diameter	0.25	mm

Maximum Ratings, Absolute-Maximum Values

Reverse Current at 22° C:

Average value, continuous operation	200	μA
Peak value (For 1 second duration, non-repetitive	1	mA

Forward Current, I_F at 22°C:

Average value, continuous operation	5	mA
Peak value (For 1 second duration, non-repetitive)	50	mA
Maximum Total Power Dissipation at 22° C	60	mW

Ambient Temperature —

Storage, T_{stg}	-60 to + 100	°C
Operating, T_A	-40 to +70	°C
Soldering:		
For 5 seconds	200	°C

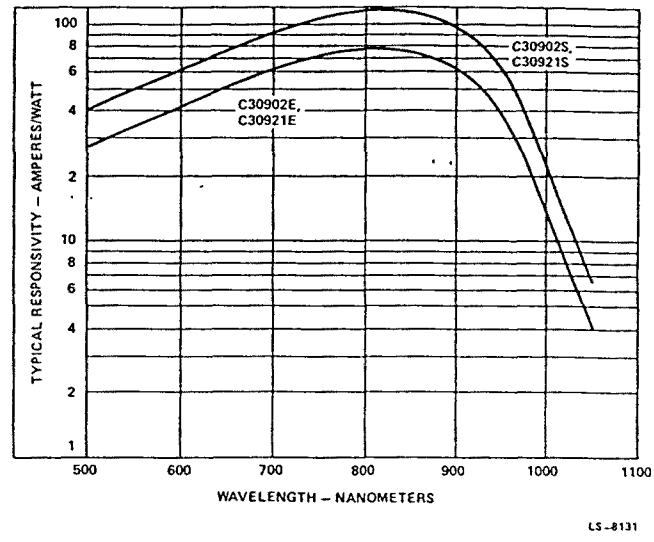

Fig. 1 Typical Spectral Responsivity at 22° C

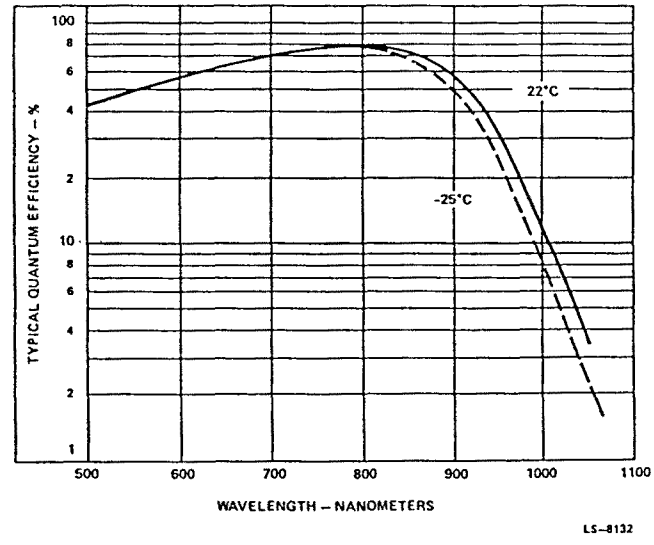

Fig. 2 Typical Quantum Efficiency vs Wavelength

Electrical Characteristics[1] at T_A = 22° C

	C30902E, C30921E			C30902S, C30921S			Units
	Min	Typ	Max	Min	Typ	Max	
Breakdown voltage V_{BR}	–	225	–	–	225	–	V
Temperature Coefficient of V_R for Constant Gain	0 5	0 7	0 8	0 5	0 7	.0 8	V/° C
Gain	–	150	–	–	250	–	
Responsivity							
At 900 nm	55	65	–	92	108	–	A/W
At 830 nm	70	77	–	117	128	–	A/W
Quantum Efficiency							
At 900 nm	–	60	–	–	60	–	%
At 830 nm	–	77	–	–	77	–	%
Dark Current I	–	1 5x10⁻⁸ (Figure 6)	3x10⁻⁸	–	1x10⁻⁸ (Figure 6)	3x10⁻⁸	A
Noise Current [2] f = 10 kHz Δ f = 1 0 Hz	–	2 3x10⁻¹⁴ (Figure 3)	5x10⁻¹⁴	–	1 1x10⁻¹⁴ (Figure 3)	2x10⁻¹⁴	A/Hz½
Capacitance C	–	1 6	2	–	1 6	2	pF
Rise Time t_r R_L = 50 Ω λ = 830 nm 10% to 90% points	–	0 5	0 75	–	0 5	0 75	ns
Fall Time R_L = 50 Ω λ = 830 nm 90% to 10% points	–	0 5	0 75	–	0 5	0 75	ns
Geiger Mode (See Appendix)							
Dark Count Rate at 5% Photon Detection Probability[3] (830 nm)							
22° C	–	–	–	–	15 000	30 000	cps
-25° C	–	–	–	–	350	700	cps
Voltage Above V_{BR} for 5% Photon Detection Probability[3] (830 nm) (see Figure 8)	–	–	–	–	2	–	V
Dead Time Per Event (See Appendix)	–	–	–	–	300	–	ns
After Pulse Ratio at 5% Photon Detection Probability (830 nm) 22° C[4]	–	–	–	–	2	15	%

1 At the DC reverse operating voltage V_R supplied with the device and a light spot diameter of 0 25 mm (C30902E, S) or 0 10 mm (C30921E, S) Note that a specific value of V_R is supplied with each device When the photodiode is operated at this voltage, the device will meet the electrical characteristic limits shown above The voltage value will be within the range of 180 to 250 volts

2 The theoretical expression for shot noise current in an avalanche photodiode is $i_n = (2q (I_{ds} + (I_{db}M^2 + P_oRM) \Gamma) B_w)^{1/2}$ where q is the electronic charge I_{ds} is the dark surface current, I_{db} is the dark bulk current Γ is the excess noise factor M is the gain P_o is the optical power on the device and B_w is the noise bandwidth For these devices $\Gamma = 0\ 98\ (2\text{-}1/M) + 0\ 02\ M$ (Reference PP Webb, RJ McIntyre, JJ Conradi, "RCA Review", Vol 35, p 234, (1974)

3 The C30902S and C30921S can be operated at a substantially higher Dectection Probabilities See Appendix

4 After-Pulse occurring 1 microsecond to 60 seconds after main pulse

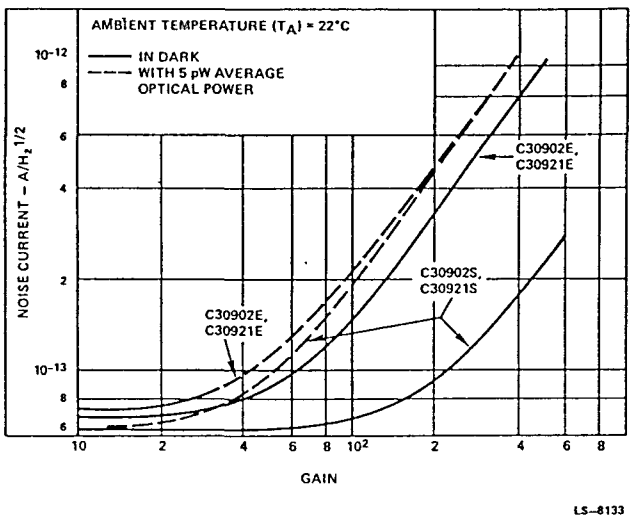

Fig. 3 Typical Noise Current vs Gain

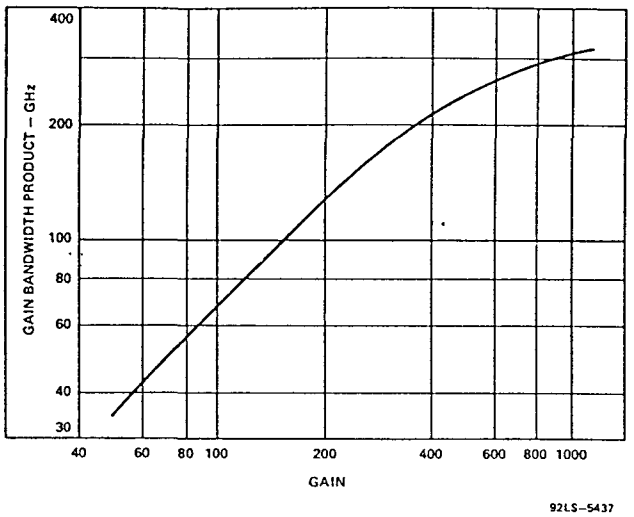

Fig. 5 Typical Gain-Bandwidth Product vs Gain

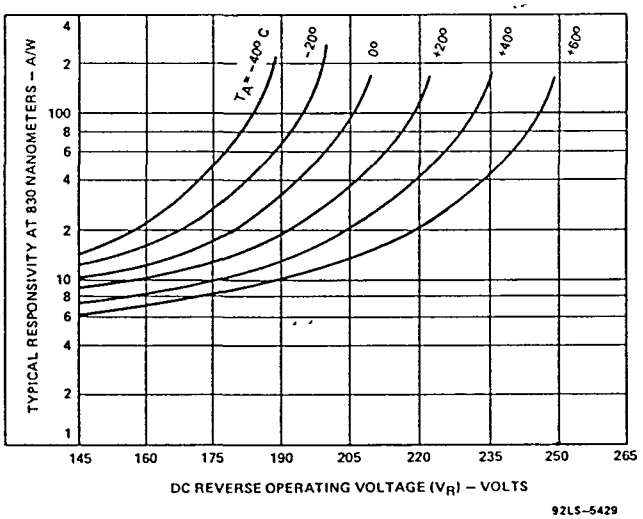

Fig. 4 Typical Responsivity at 830 nm vs Operating Voltage

Note: Operation below 145 volts is not recommended, since the device is not fully depleted below this value

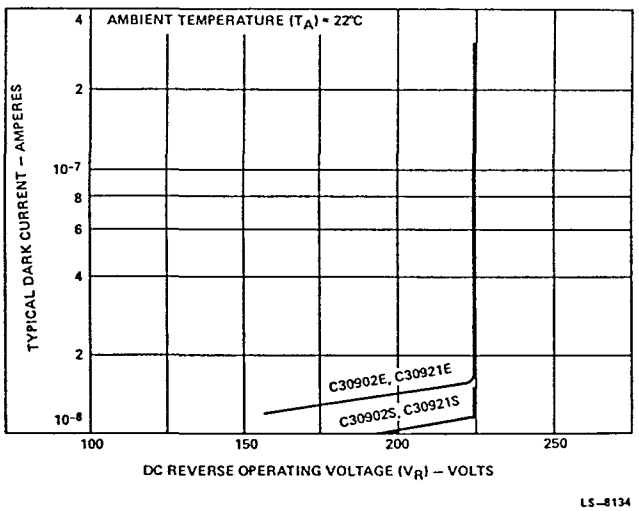

Fig. 6 Typical Dark Current vs Operating Voltage ($V<V_{BR}$)

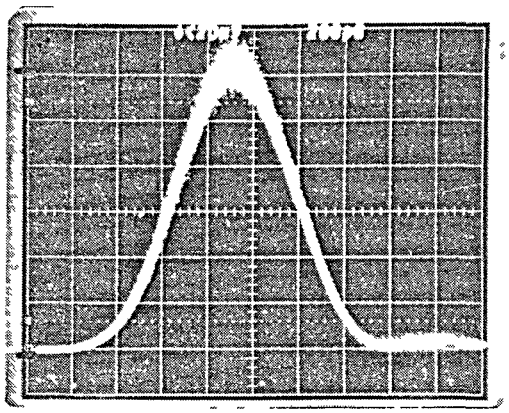

Fig. 7 Avalanche Photodiode Response to a 100 ps Laser Pulse as Measured With a 350 ps Sampling Head. (Horizontal Axis: 200 ps /Division)
Normal Linear Mode $V_R<V_{BR}$

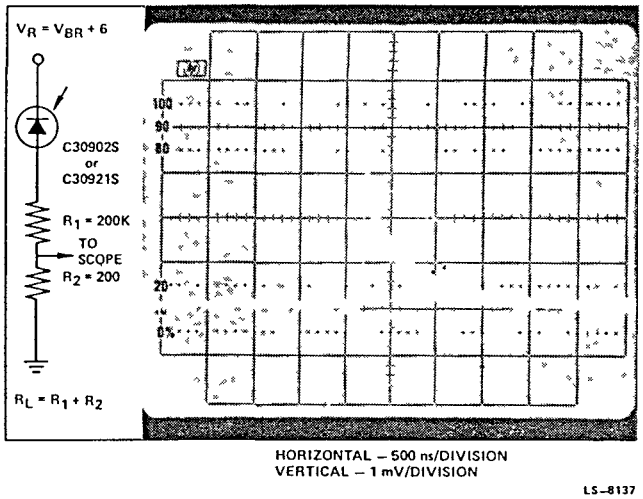

Fig. 9 Passively Quenched Circuit and Resulting Pulse Shape

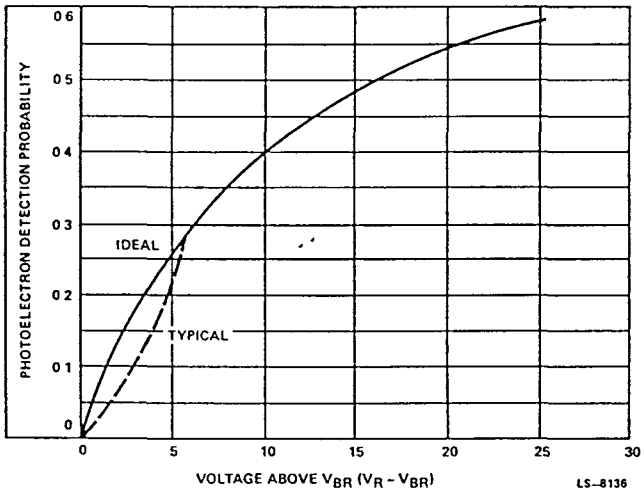

Fig. 8 Gelger Mode, Photoelectron Detection Probability vs Voltage Above V_{BR} ($V_R>V_{BR}$)

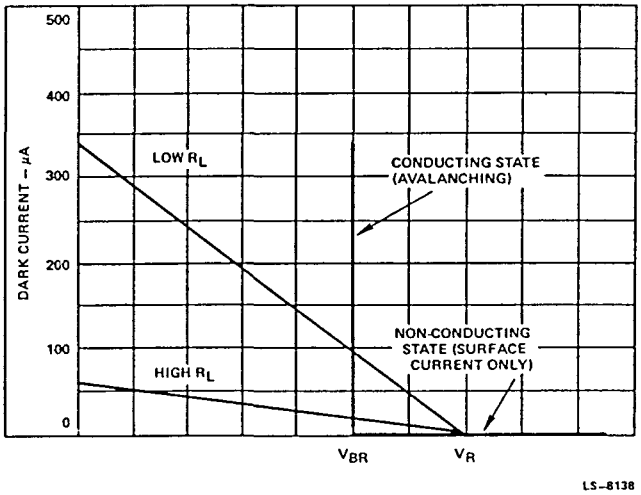

Fig. 10 Load Line for C30921S in the Geiger Mode

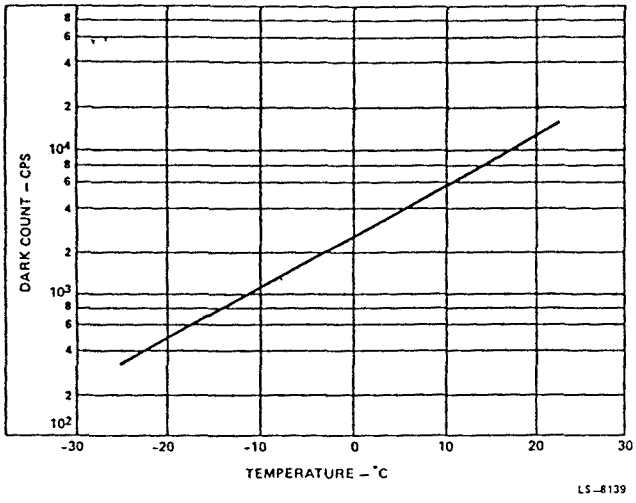

Fig. 11 Typical Dark Count vs Temperature at 5% Photon (830 nm) Detection Efficiency

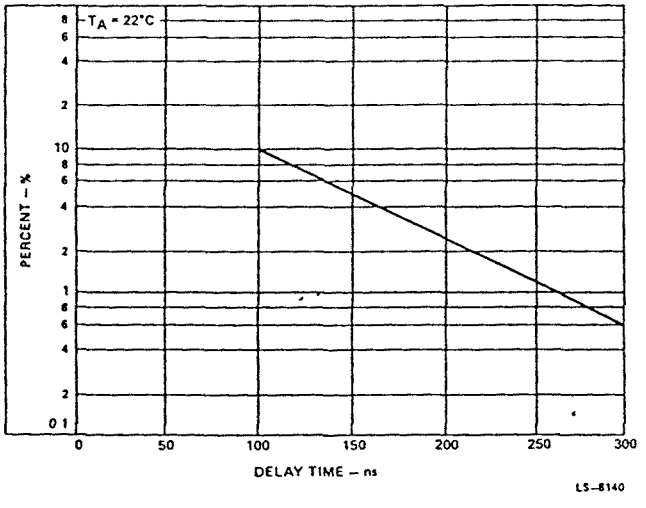

Fig. 12 Chance of an After-Pulse Within the Next 100 ns vs Delay-Time in an Actively Quenched Circuit.
(Typical for C30902S, C30921S at V_{BR} + 25)

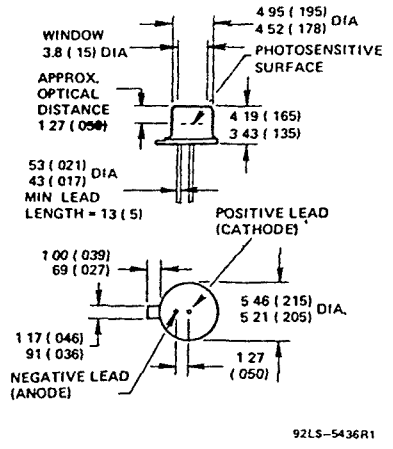

Modified TO-18 Package

Dimensions in millimeters Dimensions in parentheses are in inches.

Note: Optical distance is defined as the distance from the surface of the silicon chip to the front surface of the window.

Fig 13 Dimensional Outline - C30902E, C30902S

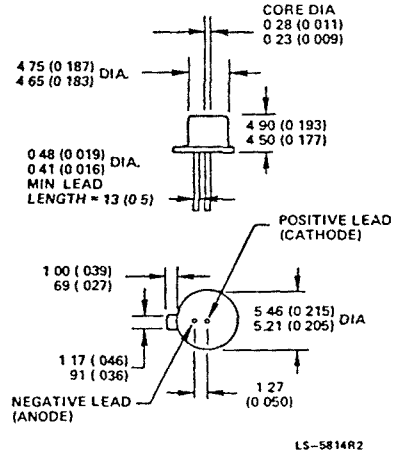

TO-18 Package

Dimensions in millimeters. Dimensions in parentheses are in inches.

Fig. 14 Dimensional Outline - C30921E, C30921S

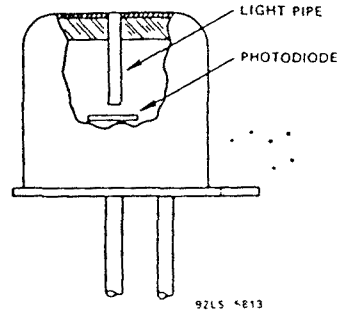

Fig. 15 Cutaway of the RCA C30921E, C30921S

A.2. Especificaciones del integrado CLC425.

Comlinear Corporation

Ultra Low Noise Wideband Op Amp

Preliminary **CLC425**

APPLICATIONS:

- instrumentation sense amplifiers
- ultrasound pre-amps
- magnetic tape & disk pre-amps
- photo-diode transimpedance amplifiers
- wide band active filters
- low noise figure RF amplifiers
- professional audio systems
- low-noise loop filters for PLLs

FEATURES (typical):

- 1.7GHz gain-bandwidth product
- 1.05nV/√Hz input voltage noise
- 1.6pA/√Hz input current noise
- 100µV input offset voltage, 2µV/°C drift
- 350V/µs slew rate
- 15mA to 5mA adjustable supply current
- gain range ±10 to ±1,000V/V
- evaluation board and simulation macromodel

DESCRIPTION

The CLC425 combines a wide bandwidth (**1.7GHz GBW**) with very low input noise (**1.05nV/√Hz, 1.6pA/√Hz**) and low dc errors (**100µV vos, 2µV/°C drift**) to provide a very precise, wide dynamic-range op amp offering closed-loop gains of ≥10.

Singularly suited for very wideband high-gain operation, the CLC425 employs a traditional voltage-feedback topology providing all the benefits of balanced inputs, such as low offsets and drifts, as well as a 96dB open-loop gain, a 100dB CMRR and a 95dB PSRR.

The CLC425 also offers great flexibility with its externally adjustable supply current, allowing designers to easily choose the optimum set of power, bandwidth, noise and distortion performance. Operating from ±5V power supplies, the CLC425 defaults to a 15mA quiescent current, or by adding one external resistor, the supply current can be adjusted to less than 5mA.

The CLC425's combination of ultra-low noise, wide gain-bandwidth, high slew rate and low dc errors will enable applications in areas such as medical diagnostic ultrasound, magnetic tape & disk storage, communications and opto-electronics to achieve maximum high-frequency signal-to-noise ratios.

The CLC425 is available in the following versions.

CLC425AJP	-40°C to +85°C	8-pin PDIP
CLC425AJE	-40°C to +85°C	8-pin SOIC
CLC425AIB	-40°C to +85°C	8-pin CerDIP
CLC425A8B	-55°C to +125°C	8-pin CerDIP, MIL-STD-883 Level B
CLC425A8L-2	-55°C to +125°C	20-pin LCC, MIL-STD-883 Level B
CLC425ALC	-55°C to +125°C	dice
CLC425AMC	-55°C to +125°C	dice, MIL-STD-883 Level B

Contact factory for other packages and DESC SMD number.

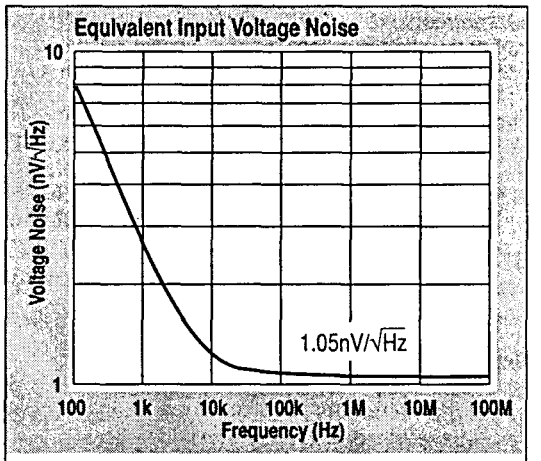

Pinout

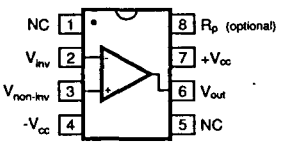

Chip Topography

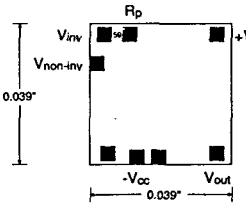

Thickness is 0.014in. Note: Backside connected to -Vcc. It is not necessary to electrically connect the backside to the negative power supply. Contact factory for more information.

Package Dimensions

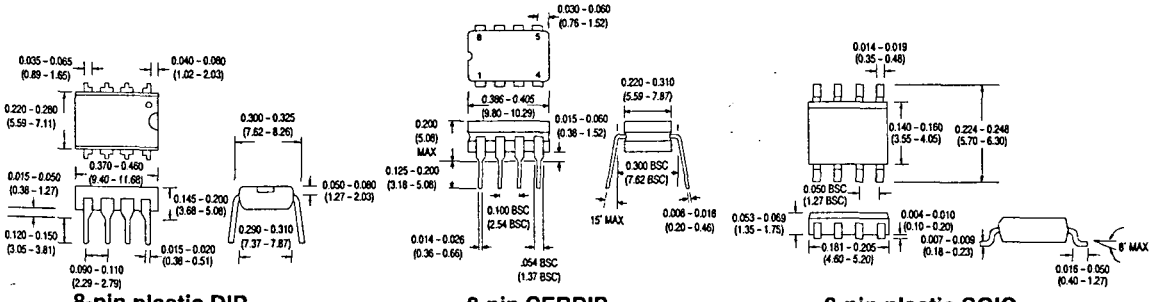

Electrical Characteristics

PARAMETERS	CONDITIONS	TYP	MIN AND MAX RATINGS			UNITS	SYMBOL
Ambient Temperature	CLC425 AJ/AI	+25°C	-40°C	+25°C	+85°C		
Ambient Temperature	CLC425 A8/AM/AL	+25°C	-55°C	+25°C	+125°C		
FREQUENCY DOMAIN RESPONSE							
gain bandwidth product	V_{out} < 0.4V_{pp}	1.7				GHz	GBW
†-3dB bandwidth	V_{out} < 0.4V_{pp}	85	TBD	TBD	TBD	MHz	SSBW
	V_{out} < 5.0V_{pp}	TBD	TBD	TBD	TBD	MHz	LSBW
gain flatness	V_{out} < 0.4V_{pp}						
† peaking	DC to 30MHz	0.3	TBD	TBD	TBD	dB	GFP
† rolloff	DC to 30MHz	0.1	TBD	TBD	TBD	dB	GFR
linear phase deviation	DC to 30MHz	TBD	TBD	TBD	TBD	°	LPD
TIME DOMAIN RESPONSE							
rise and fall time	0.4V step	4.1	TBD	TBD	TBD	ns	TRS
settling time to 0.1%	2V step	22	TBD	TBD	TBD	ns	TSS
overshoot	0.4V step	5	TBD	TBD	TBD	%	OS
slew rate	2V step	350	TBD	TBD	TBD	V/µs	SR
DISTORTION AND NOISE RESPONSE							
†2nd harmonic distortion	1V_{pp}, 10MHz	- 50	TBD	TBD	TBD	dBc	HD2
†3rd harmonic distortion	1V_{pp}, 10MHz	- 80	TBD	TBD	TBD	dBc	HD3
3rd order intermodulation intercept	10MHz	35				dBm	IMD
1/f input voltage noise corner		500				Hz	1/F
equivalent noise input							
voltage	TBD to 100MHz	1.05	TBD	TBD	TBD	nV/√Hz	VN
current	TBD to 100MHz	1.6	TBD	TBD	TBD	pA/√Hz	ICN
noise floor	TBD to 100MHz	- 165	TBD	TBD	TBD	dBm_{1Hz}	SNF
integrated noise	TBD to 100MHz	12	TBD	TBD	TBD	µV	INV
STATIC DC PERFORMANCE							
open-loop gain	DC	96	77	86	86	dB	AOL
*input offset voltage		± 100	± 1000	± 800	± 1000	µV	VIO
average drift		± 2	8	—	4	µV/°C	DVIO
*input bias current		12	34	20	20	µA	IB
average drift		- 100	- 250	—	- 120	nA/°C	DIB
input offset current		± 0.2	3.4	2.0	2.0	µA	IIO
average drift		± 3	± 50	—	± 25	nA/°C	DIIO
†power supply rejection ratio	DC	95	82	88	88	dB	PSRR
♠common mode rejection ratio	DC	100	88	92	92	dB	CMRR
*supply current	R_L= ∞	15	18	16	16	mA	ICC
MISCELLANEOUS PERFORMANCE							
input resistance	common-mode	2	0.6	1.6	1.6	MΩ	RINC
	differential-mode	6	1	3	3	kΩ	RIND
input capacitance	common-mode	2.5	3	3	3	pF	CINC
output resistance	closed loop	5	50	10	10	mΩ	ROUT
output voltage range	R_L= ∞	± 3.8	± 3.5	± 3.7	± 3.7	V	VO
	R_L=100Ω	± 3.4	± 2.8	± 3.2	± 3.2	V	VOL
input voltage range	common mode	± 3.8	± 3.4	± 3.5	± 3.5	V	CMIR
output current	source -55°C/-40°C	90	60/70	70	70	mA	IOP
	sink -55°C/-40°C	90	40/55	55	55	mA	ION

Absolute Maximum Ratings

V_{cc}	±7V
I_{out} short circuit protected to ground, however maximum reliability is obtained if I_{out} does not exceed...	150mA
common-mode input voltage	±V_{cc}
differential input current diode protected	±25mA
maximum junction temperature	+175°C
operating temperature range	
AJ/AI	-40°C to +85°C
A8/ AM/AL:	-55°C to +125°C
storage temperature range	-65°C to +150°C
lead temperature (soldering 10 sec)	+300°C

Notes

Recommended gain range ±10 to ±1,000V/V

Notes:

* AJ,AI : 100% tested at +25°C, sample at +85°C.
† AJ : Sample tested at +25°C.
† AI : 100% tested at +25°C.
* A8 : 100% tested at +25°C, -55°C, +125°C.
† A8 : 100% tested at +25°C, sample at -55°C, +125°C
* AL, AM : 100% wafer probed +25°C to +25°C min/max specs.
♠ SMD : Sample tested at +25°C, -55°C and +125°C.

CLC425 Typical Performance (T_A = 25°C, V_{CC} = ±5V, R_L = 26 Ω, R_F = 499 Ω, R_G = 100 Ω unless noted)

Non-Inverting Frequency Response

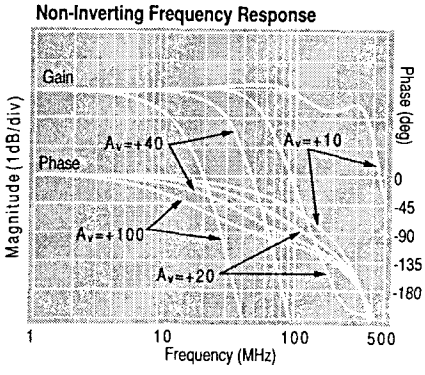

Inverting Frequency Response

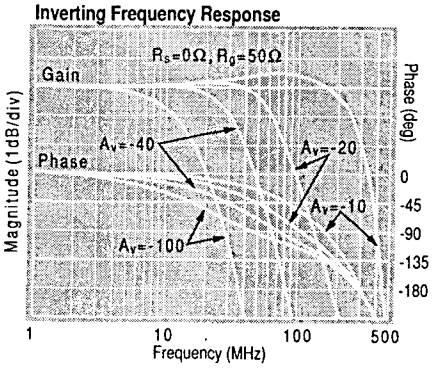

Frequency Response vs. I_{CC} (A_V=+20)

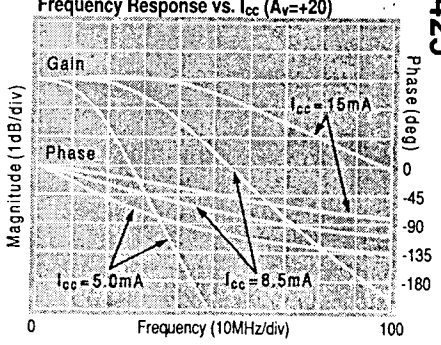

Open Loop Gain and Phase vs. I_{CC}

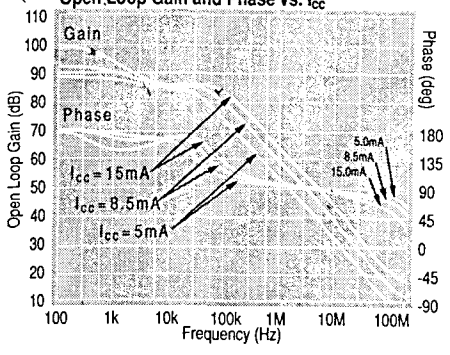

Open Loop Gain and Phase vs. R_L

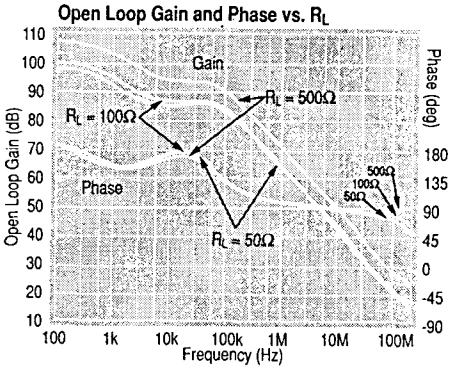

Open Loop Gain and Phase vs. Temp

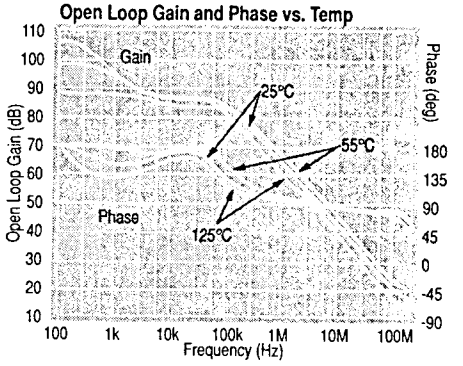

Non-Inverting Response (I_{CC}=5.0mA)

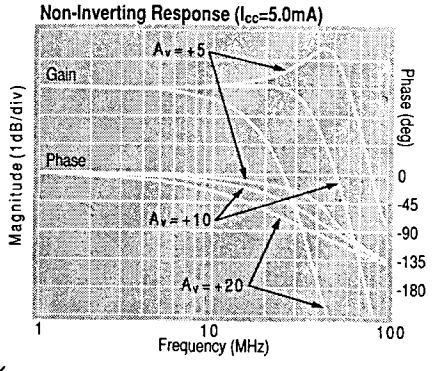

Frequency Response for Various R_Ls

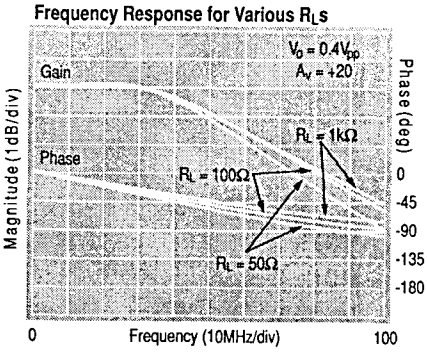

Gain Flatness & Linear Phase Deviation

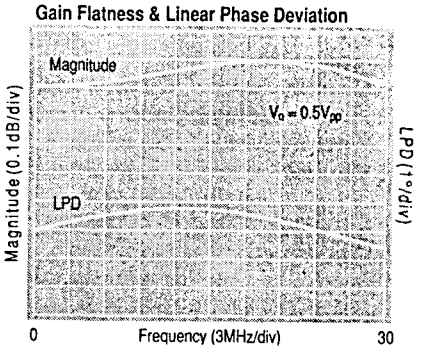

Equivalent Input Noise

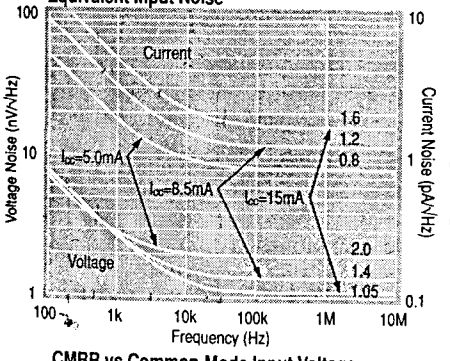

Maximum Output Swing vs. Frequency

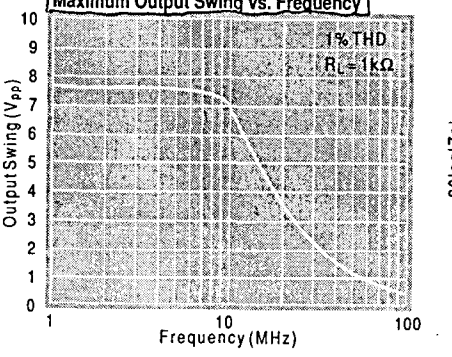

Closed-Loop Output Impedance

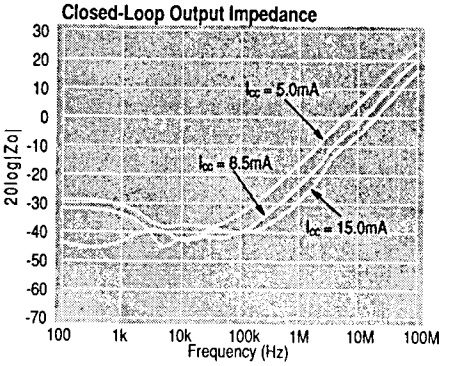

CMRR vs Common-Mode Input Voltage

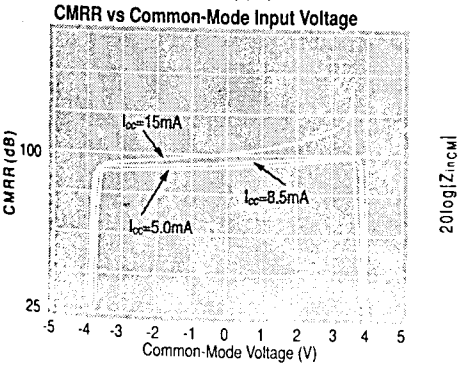

Common Mode Input Impedance

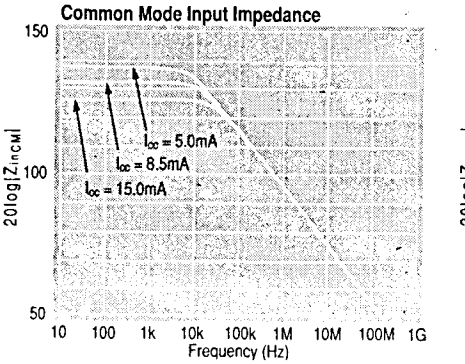

Differential Input Impedance

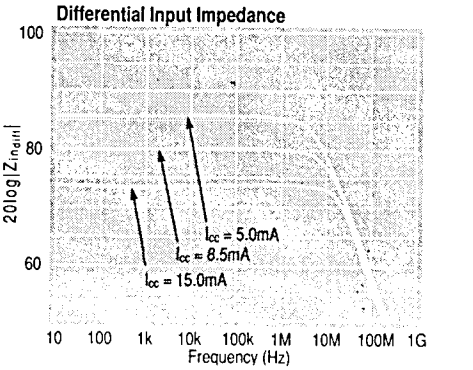

CLC425 Typical Performance (T_A = 25°C, V_{CC} = ±5V, R_S = 25Ω, R_F = 499Ω, R_L = 100Ω unless noted)

Pulse Response (V_O=1V_{pp})

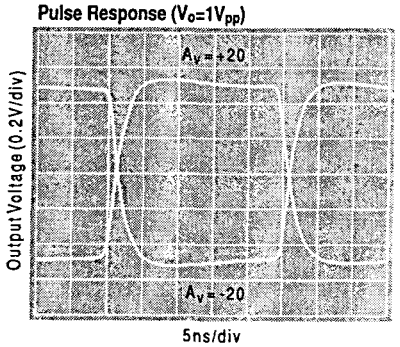

Large Signal Pulse Response (V_O=2V_{pp})

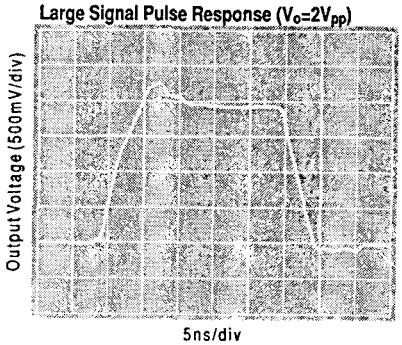

Settling Time vs. Gain

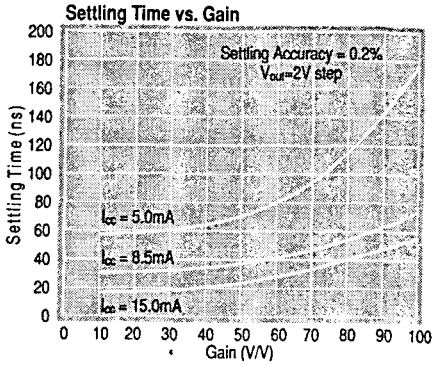

Short Term Settling Time

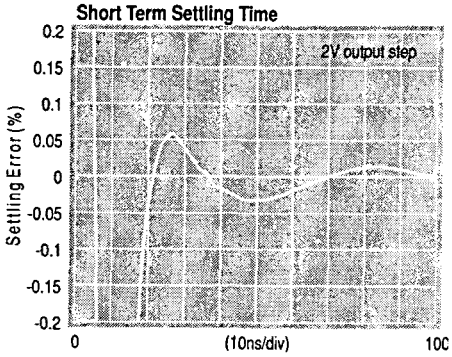

Long Term Settling Time

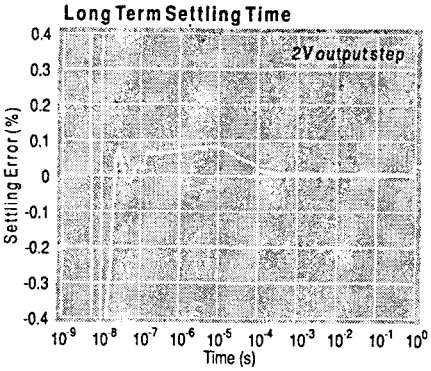

Settling Time vs. C_L and R_S

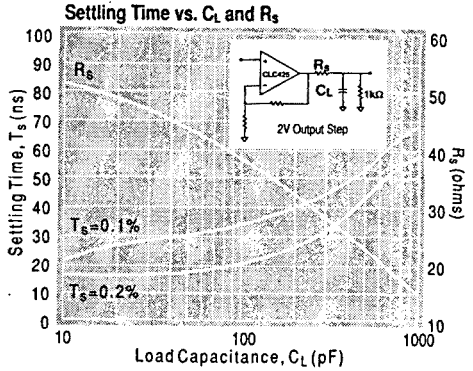

Supply Current Range vs. Rp

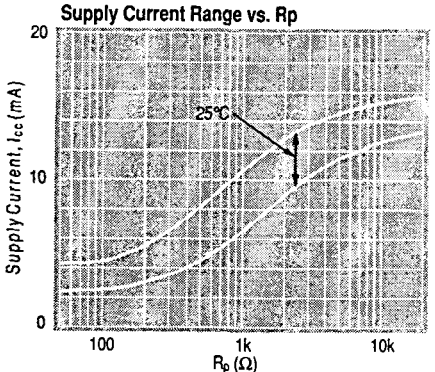

Gain-Bandwidth Product vs I_{cc}

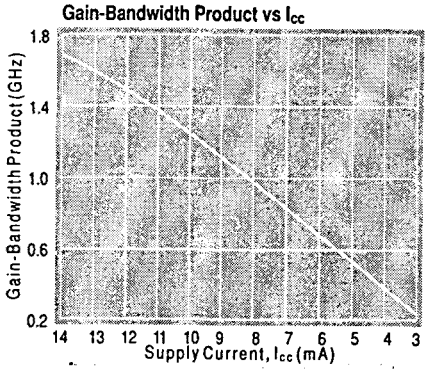

Differential Gain and Phase (4.43MHz)

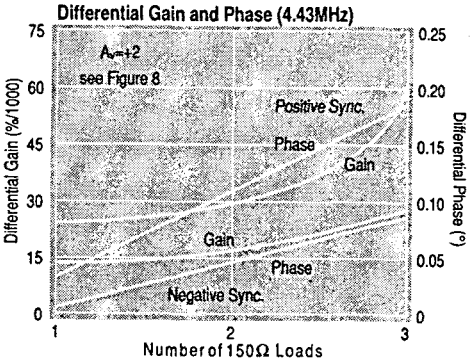

2nd and 3rd Harmonic Distortion (V_O=1V_{pp})

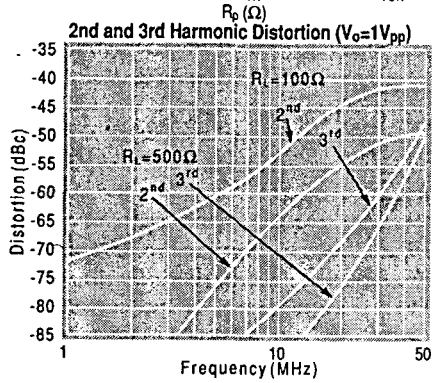

Distortion vs. Gain & I_{cc} (V_O=1V_{pp}, f_O=3MHz)

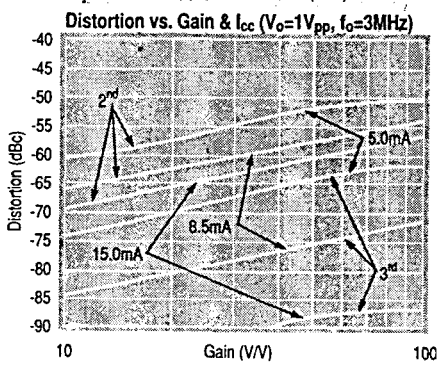

2-Tone, 3rd Order Intermodulation Intercept

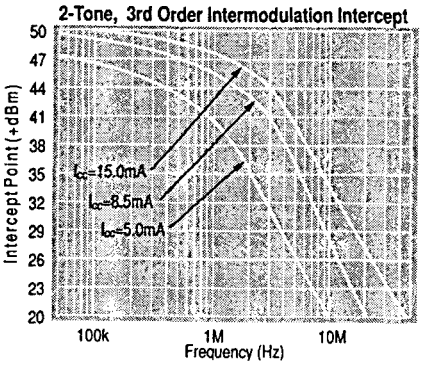

Output Voltage vs Load

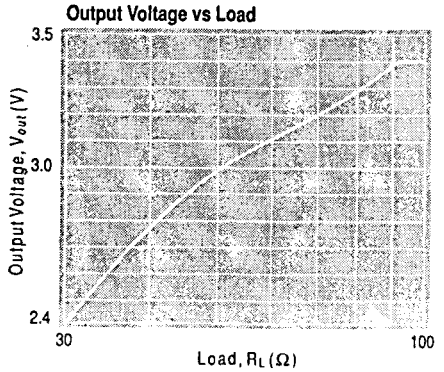

CMRR and PSRR

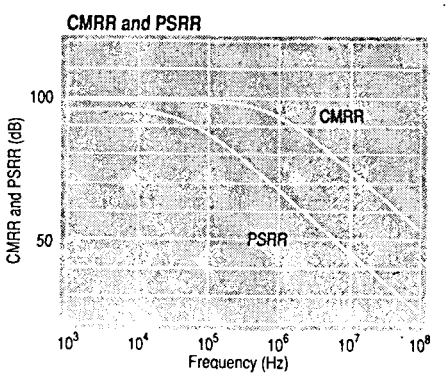

Typical DC Errors vs. Temperature

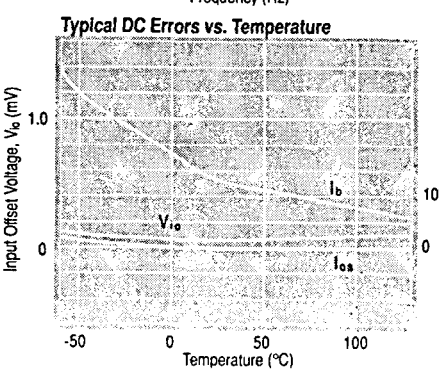

A.3. Expresión completa de la ecuación algebraica II.15.

```
A2*B1^2*C2 + B1*B2*C2*D1 + A2*B1*D1*D2 + B2*D1^2*D2 + B1^2*C2^2*d3 +
 2*B1*C2*D1*D2*d3 + D1^2*D2^2*d3 +
 d1^4*(A2*C1^2*C2 + C1^2*C2^2*d3) + 2*A2*B1*C2*D1*K + B2*C2*D1^2*K +
 A2*D1^2*D2*K + 2*B1*C2^2*D1*d3*K + 2*C2*D1^2*D2*d3*K +
 A2*C2*D1^2*K^2 + C2^2*D1^2*d3*K^2 +
 d1^3*(-2*A1*A2*C1*C2 - B2*C1^2*C2 + 2*A2*C1*C2*D1 - A2*C1^2*D2 -
    2*A1*C1*C2^2*d3 + 2*C1*C2^2*D1*d3 - 2*C1^2*C2*D2*d3 -
    2*A2*C1^2*C2*K - 2*C1^2*C2^2*d3*K) + A1^2*A2*C2*z0^2 +
 A1*B2*C1*C2*z0^2 + A1*A2*C1*D2*z0^2 + B2*C1^2*D2*z0^2 +
 A1^2*C2^2*d3*z0^2 + 2*A1*C1*C2*D2*d3*z0^2 + C1^2*D2^2*d3*z0^2 +
 2*A1*A2*C1*C2*K*z0^2 + B2*C1^2*C2*K*z0^2 + A2*C1^2*D2*K*z0^2 +
 2*A1*C1*C2^2*d3*K*z0^2 + 2*C1^2*C2*D2*d3*K*z0^2 +
 A2*C1^2*C2*K^2*z0^2 + C1^2*C2^2*d3*K^2*z0^2 +
 d1^2*(A1^2*A2*C2 - 2*A2*B1*C1*C2 + A1*B2*C1*C2 - 2*A1*A2*C2*D1 -
    2*B2*C1*C2*D1 + A2*C2*D1^2 + A1*A2*C1*D2 + B2*C1^2*D2 -
    2*A2*C1*D1*D2 + A1^2*C2^2*d3 - 2*B1*C1*C2^2*d3 -
    2*A1*C2^2*D1*d3 + C2^2*D1^2*d3 + 2*A1*C1*C2*D2*d3 -
    4*C1*C2*D1*D2*d3 + C1^2*D2^2*d3 + 2*A1*A2*C1*C2*K +
    B2*C1^2*C2*K - 4*A2*C1*C2*D1*K + A2*C1^2*D2*K +
    2*A1*C1*C2^2*d3*K - 4*C1*C2^2*D1*d3*K + 2*C1^2*C2*D2*d3*K +
    A2*C1^2*C2*K^2 + C1^2*C2^2*d3*K^2 + A2*C1^2*C2*z0^2 +
    C1^2*C2^2*d3*z0^2) + d1*
  (2*A1*A2*B1*C2 + B1*B2*C1*C2 - 2*A2*B1*C2*D1 + A1*B2*C2*D1 -
    B2*C2*D1^2 + A2*B1*C1*D2 + A1*A2*D1*D2 + 2*B2*C1*D1*D2 -
    A2*D1^2*D2 + 2*A1*B1*C2^2*d3 - 2*B1*C2^2*D1*d3 +
    2*B1*C1*C2*D2*d3 + 2*A1*C2*D1*D2*d3 - 2*C2*D1^2*D2*d3 +
    2*C1*D1*D2^2*d3 + 2*A2*B1*C1*C2*K + 2*A1*A2*C2*D1*K +
    2*B2*C1*C2*D1*K - 2*A2*C2*D1^2*K + 2*A2*C1*D1*D2*K +
    2*B1*C1*C2^2*d3*K + 2*A1*C2^2*D1*d3*K - 2*C2^2*D1^2*d3*K +
    4*C1*C2*D1*D2*d3*K + 2*A2*C1*C2*D1*K^2 + 2*C1*C2^2*D1*d3*K^2 -
    2*A1*A2*C1*C2*z0^2 - B2*C1^2*C2*z0^2 - A2*C1^2*D2*z0^2 -
    2*A1*C1*C2^2*d3*z0^2 - 2*C1^2*C2*D2*d3*z0^2 -
    2*A2*C1^2*C2*K*z0^2 - 2*C1^2*C2^2*d3*K*z0^2)=0
```

A.4. Esquema eléctrico del buscador de portadora.

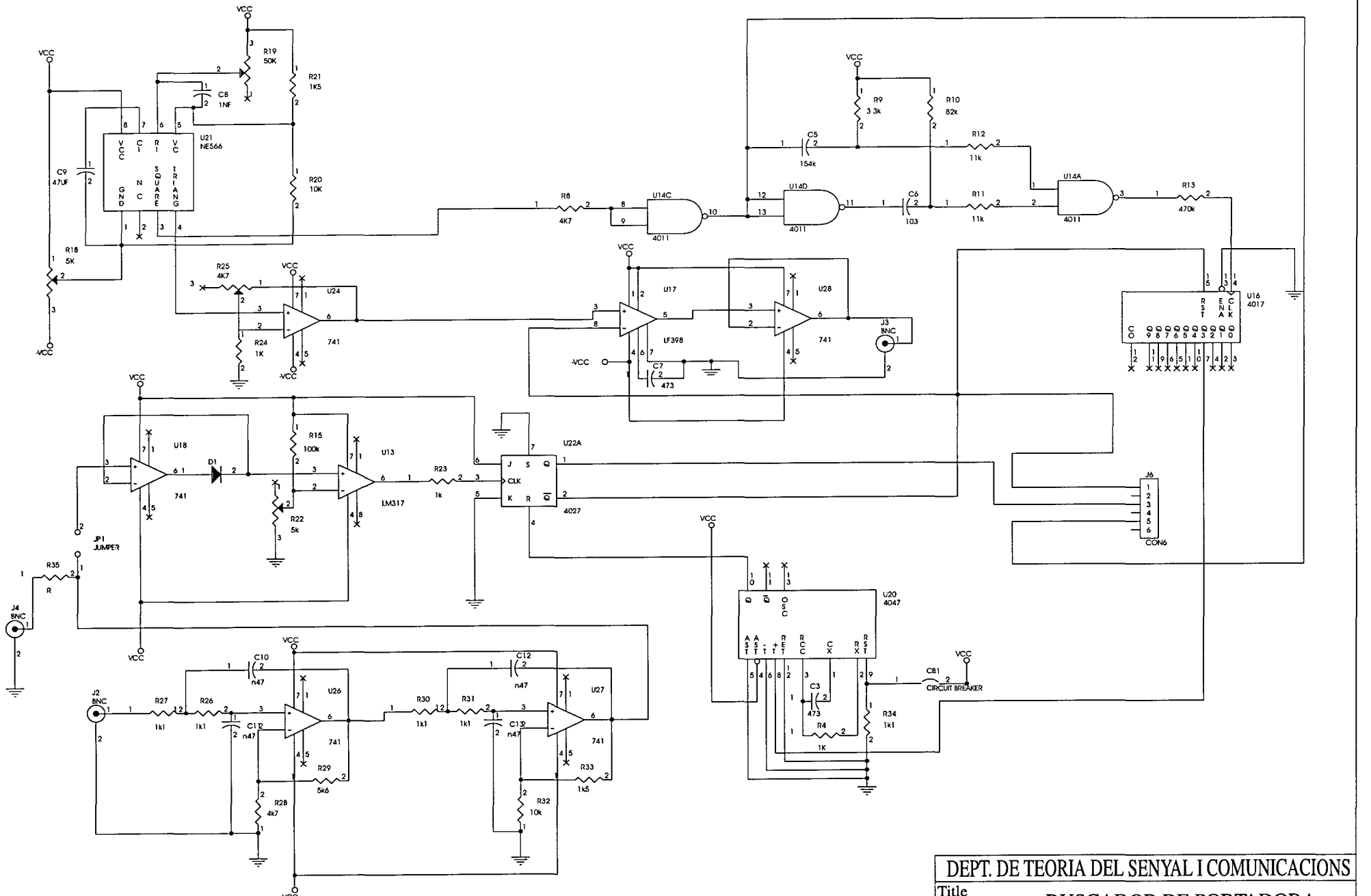

DEPT. DE TEORIA DEL SENYAL I COMUNICACIONS		
Title	BUSCADOR DE PORTADORA	
Size: C	Document Number: MESALLES 01	REV: 33
Date: July 8, 1998	Sheet 1 of 1	

A.5. Esquema eléctrico del bloque contador de frecuencia.

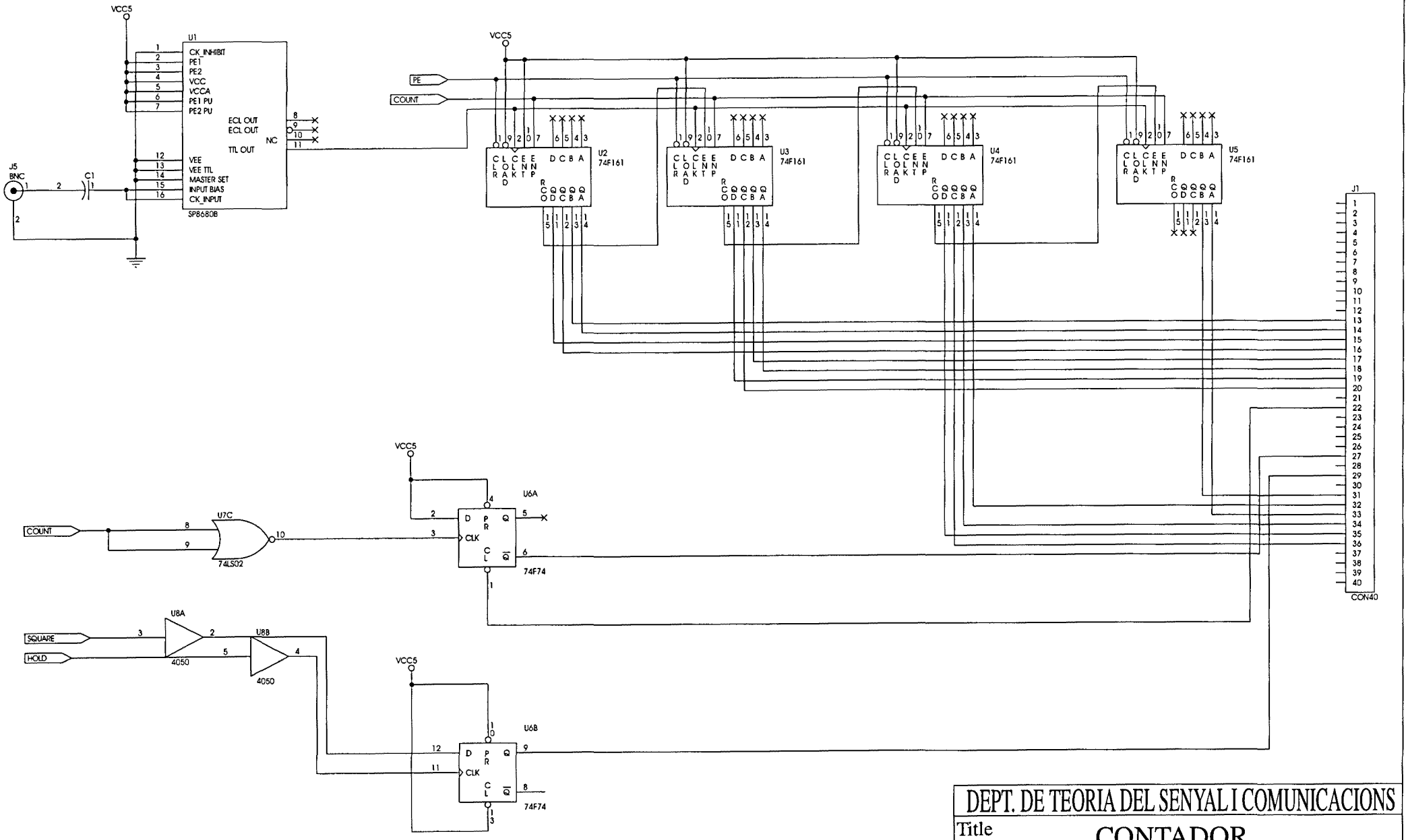

DEPT. DE TEORIA DEL SENYAL I COMUNICACIONS

Title	CONTADOR	
Size: B	Document Number: MESALLES 02	REV: 26
Date: July 8, 1998	Sheet 1 of 1	

A.6. Programa LabView™ del subsistema de adquisición, medida y presentación del lidar coherente.

elfrecuencimetro.vi
Last modified on 7/05/98 at 17:04
Printed on 14/07/98 at 11:13

Connector Pane

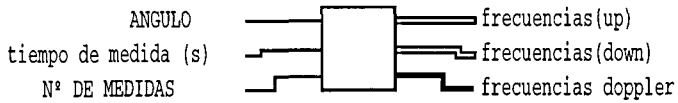

C:\Usuaris\Eloy\board\elfrecuencimetro.vi

Block Diagram

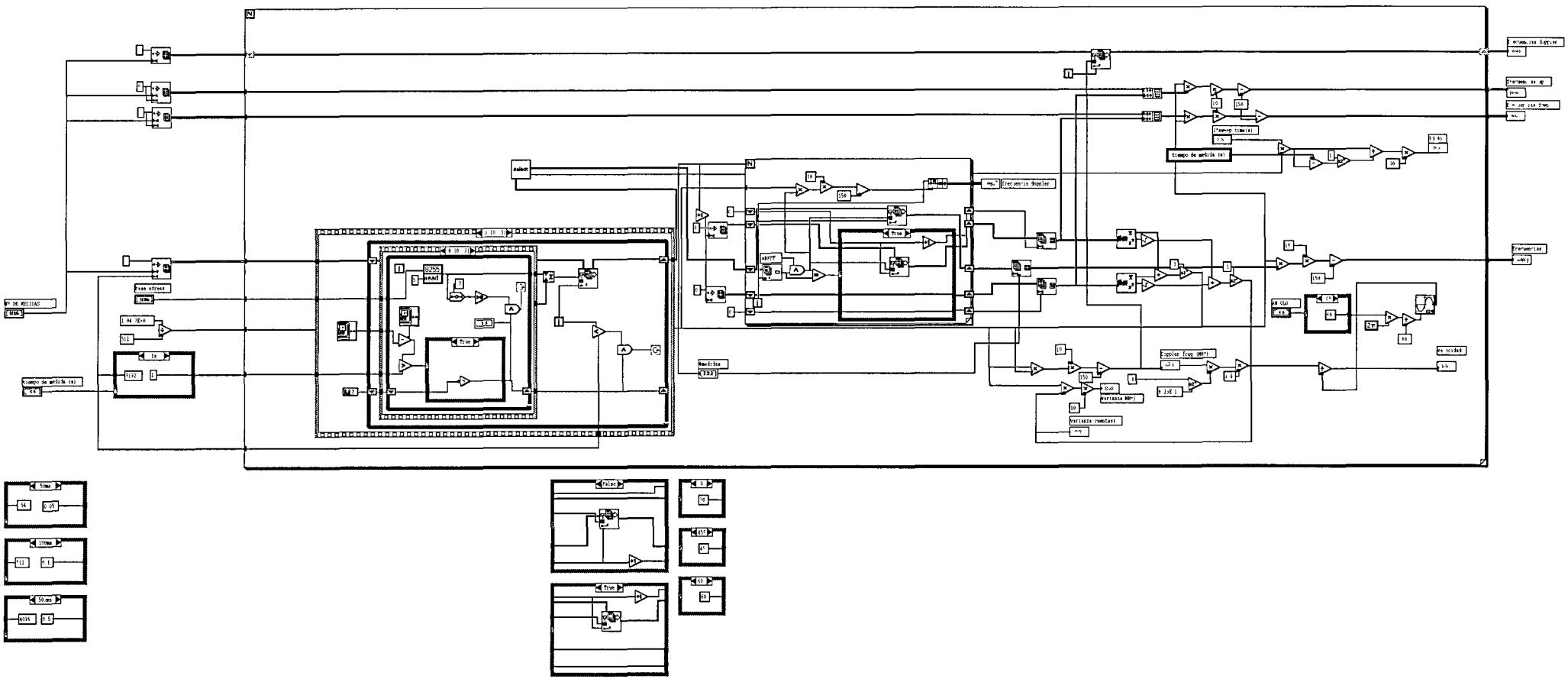

elfrecuencimetro.vi
Last modified on 7/05/98 at 17:04
Printed on 14/07/98 at 11:10

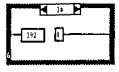

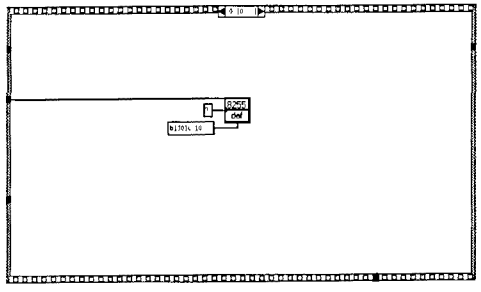

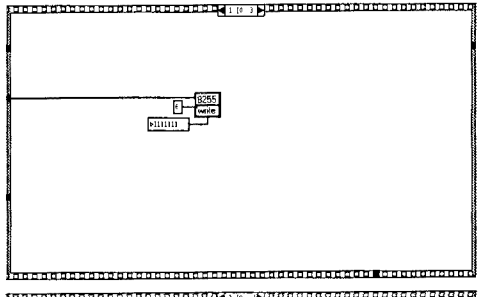

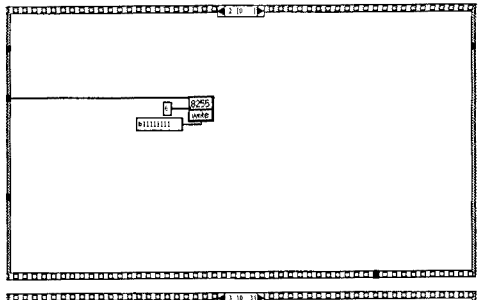

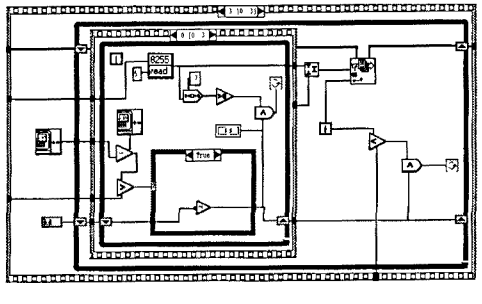

elfrecuencimetro.vi
Last modified on 7/05/98 at 17:04
Printed on 14/07/98 at 11:10

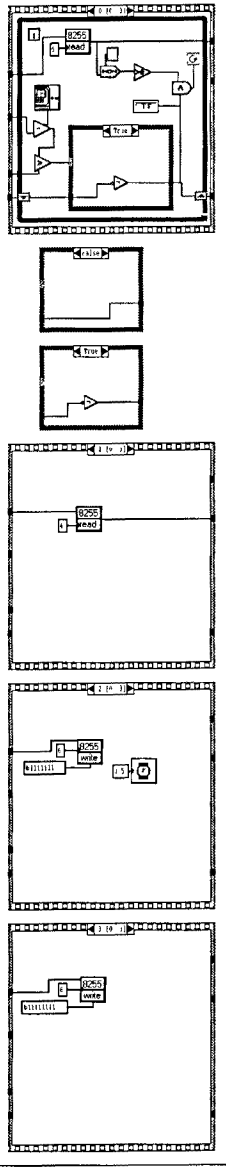

Position in Hierarchy

elfrecuencimetro.vi
Last modified on 7/05/98 at 17:04
Printed on 14/07/98 at 11:10

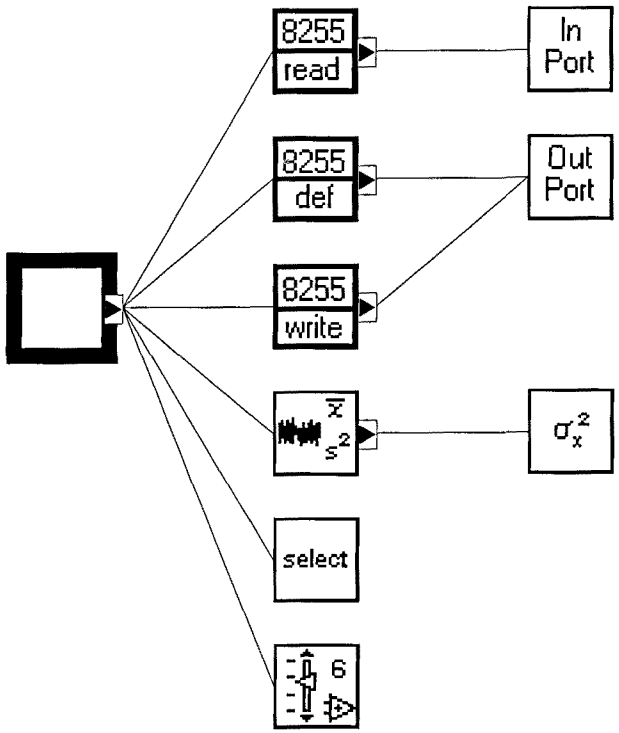

A.7. Especificaciones del diodo láser SDL-2100-E1.

1 Watt Pulsed GaAlAs Laser Diodes

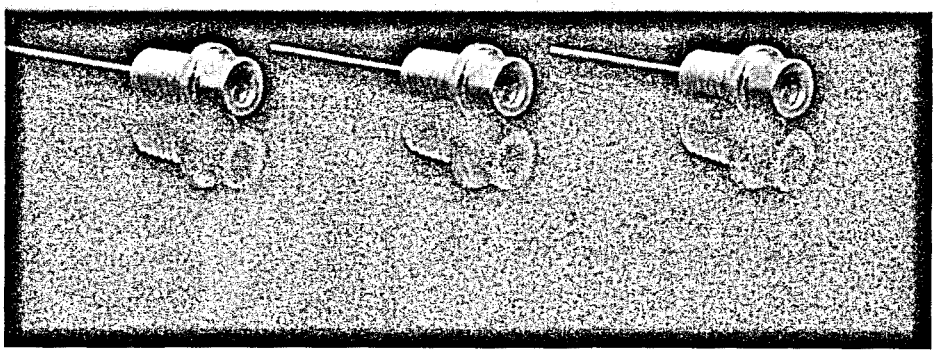

SDL-2100 Series

Features

1 W Peak Pulsed Power

High Efficiency, Low Threshold

1% Duty Factor, 10 mW Average Power

High Temperature Operating Capability

The high duty factor, high optical power offered by the SDL-2100 Series is achieved by a quantum well active layer structure that provides low threshold and highly efficient operation. An electrical-to-optical power conversion efficiency of 20% is typical. These quantum well devices feature a broad area emitter with 100 µm aperture mounted "p" up.

These devices are produced using state-of-the-art metalorganic chemical vapor deposition (MOCVD) techniques, providing reliable, long life operation over a wide range of temperatures. Greater than 10,000 hour life has been demonstrated at 1 W power, 100 ns pulse width, at 125°C case temperature.

The SDL-2100-E1 is a hermetically sealed TO-18 window package laser. The multimode beam is useful for applications including time of flight ranging, proximity detection, illumination, robotic vision and point-to-point communications. The high duty factor and high repetition rate provide 10 mW average power for integrating detectors.

The convenient TO-18 package is compatible with standard electronic fixturing and allows easy mounting in system applications.

SDL®

SDL-2100 Series Specifications

(Typical values at 25 °C and 0.6 NA collection optics)

Model Number	Peak Pulsed Power (W)	Differential Quantum Efficiency (mW/mA)	Total Conversion Efficiency (%)	Emitting Dimensions W X H (µm)	Beam Divergence $\theta_{\perp}$, $\theta_{//}$ (deg FWHM)	Threshold Current (A)	Operating Current (A)
SDL-2100-E1	**1.0**	**0.80 (50%)**	**20**	**100 x 1**	**32, 12**	**0.4**	**1.5**

Notes

1 Features common to all SDL 2100 Series laser diodes include

- a Duty Factor of 1%
- b Spectral width of 2 nm FWHM
- c Maximum Pulse Width is 100 nsec
- d Temperature coefficient of wavelength is approximately 0 27 to 0 3 nm per °C
- e Temperature coefficient of threshold current can be modeled as

  $I_{TH2} = I_{TH1} \exp [(T_2 - T_1)/T_o]$

  where T_o is a device constant of about 150
- f Temperature coefficient of operating current is approximately 0 5 to 0 7% per °C

2 Forward Voltage is typically $V_f = 1\ 5\ V + I_{op} \times R_S$

3 Wavelength range of pulsed laser diodes is 830 ± 30 nm Wavelength selection is available as an option Refer to Price List for wavelength selection range variance and price

Optical Characteristics

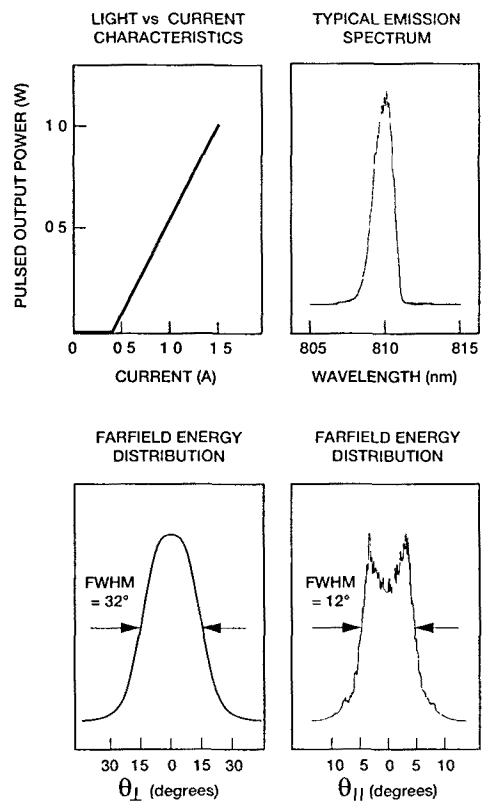

Absolute Maximum Ratings

Series Resistance (Ω)	Forward Voltage at 100 mA (volts)	Recommended Case Temperature (°C)	Peak Pulsed Power (W)	Reverse Voltage (volts)	Case Operating Temperature (°C)	Storage Temperature Range (°C)	Lead Soldering Temperature (°C for 5 sec)
0.30	1.6	0 to 30	1.1	3.0	-20 to 70	-55 to 80	250

Package Specifications [Dimensions in inches (mm) except where indicated]

SDL Standard Tolerances: (unless otherwise specified) **inches:** x xx = ±0 02, x xxx = ±0 010 **mm:** x x = ±0 5, x xx = ±0 25

E1 TO-18 WINDOW PACKAGE

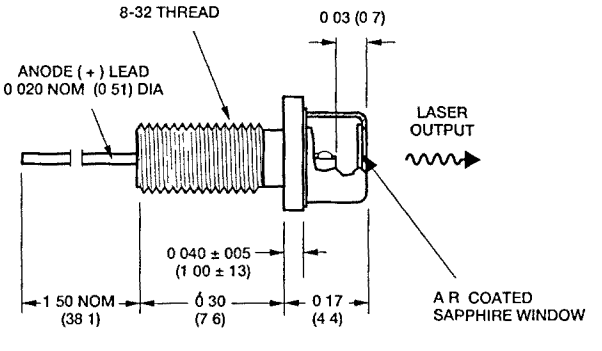

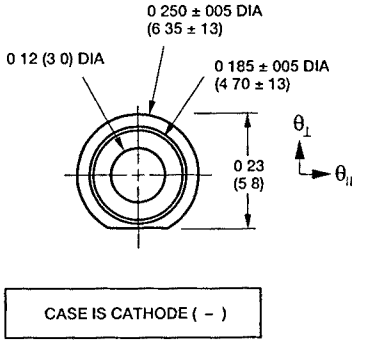

Safety And Operating Considerations

The laser light emitted from this laser diode is invisible and may be harmful to the human eye Avoid looking directly into the laser diode into the collimated beam along its optical axis when the device is in operation

CAUTION THE USE OF OPTICAL INSTRUMENTS WITH THIS PRODUCT WILL INCREASE EYE HAZARD

Operating the laser diode outside of its maximum ratings may cause device failure or a safety hazard Power supplies used with the component must be employed such that the maximum peak optical power cannot be exceeded CW laser diodes may be damaged by excessive drive current or switching transients When using power supplies the laser diode should be connected with the main power on and the output voltage at zero The current should be increased slowly while monitoring the laser diode output power and the drive current

Thermal device degradation accelerates approximately as exp (-0 7eV/kT_C) and therefore careful attention to minimize the case temperature is advised For example life expectancy will decrease by a factor of 5 if the case is operated at 50°C rather than 30°C

A proper heat sink for the laser diode on a thermal radiator will greatly enhance laser life Firmly mount the laser on a radiator having a thermal impedance of less than 5 0 °C/W for increased reliability

ESD PROTECTION — Electro-static discharge is the primary cause of unexpected laser diode failure Take extreme precaution to prevent ESD Use wrist straps, grounded work surfaces, and rigorous anti-static techniques when handling laser diodes

21 CFR 1040.10 Compliance

Because of the small size of these devices each of the labels shown is attached to the individual shipping container They are illustrated here to comply with 21 CFR 1040 10 as applicable under the radiations control for health and safety act of 1968

SERIAL NUMBER IDENTIFICATION LABEL

SDL, INC.
SAN JOSE CALIFORNIA 95134 U S A

MODEL	S/N
MANUFACTURED	
WAVELENGTH	Iop

This laser product complies with 21 CFR 1040 as applicable

OUTPUT POWER DANGER LABEL

PACKAGE APERTURE LABELS

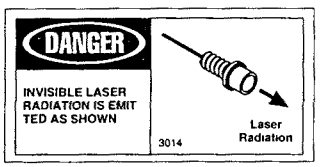

"E1" PACKAGE DIODES

In the United States and North America please contact:

SDL Inc
80 Rose Orchard Way
San Jose CA 95134 1365
TEL 408 943 9411
FAX 408 943 1070

For other distributors please call:

Argentina	Australia	Belgium	Brazil	Germany	India
Laseroptics SA	Coherent Scientific	Landre Intechmij	AMS Electronic	AMS Optotech	Laser Spectra
1 372 7547	8 352 1111	3 887 0 05	1 69 07 02 54	89 12 68 060	806 609 342
Israel	Italy	Japan	Netherlands	PRC	Poland Hungary
Isramex	BFI Ibexsa	Marubun Corp	ACAL Auriema	Superbin	RBM R Braumann
3 647 4440	2 3310 0535	3 3639 9811	40 502 602	1 499 3970	89 156 011
Portugal Spain	Scandinavia	Singapore	Switzerland	Taiwan	UK
Photonetics Espana	Gamma Optronik	PDM Technologies	GMP SA	Banin Enter	AMS Electronic
1 677 7753	18 555 885	11 788 0806	21 634 8181	2 917 2071	245 496 212